



WPI

Project ID: SA2-2103

Spring-Loaded Needle Delivery System of Cells into Decellularized Scaffold

A Major Qualifying Project Report submitted to the faculty of
WORCESTER POLYTECHNIC INSTITUTE
in partial fulfillment of the requirements for the degree of Bachelor of Science.

This report represents the work of one or more WPI undergraduate students
submitted to the faculty as evidence of completion of a degree requirement.
WPI routinely publishes these reports on the web without editorial or peer review.

Submitted by:

Alexandria Baker

Cosette Domkofski

Minh Anh Kieu

Siri Sundaraneedi

Submission Date April 27th, 2022

Professor Sakthikumar, Ambady, Ph.D., Advisor
Department of Biomedical Engineering

Table of Contents

| | |
|---|----|
| Table of Contents | 2 |
| Authorship | 4 |
| Acknowledgements | 5 |
| Abstract | 6 |
| Chapter 1: Introduction | 7 |
| Chapter 2: Literature Review | 8 |
| Decellularization of Natural Tissue | 8 |
| A Potential Application: Cardiac Grafts and Transplants | 9 |
| Microneedles | 10 |
| Prior Arts: Gold Standard: Clemson Study | 11 |
| Prior Arts: Cell Seeding Techniques | 11 |
| Chapter 3: Project Strategy | 13 |
| 3.1 Initial Client Statement | 13 |
| 3.2 Design Requirements (Technical) | 13 |
| 3.3 Design Requirements (Standards) | 13 |
| 3.4 Revised Client Statement | 14 |
| 3.5 Management Approach | 14 |
| Chapter 4: Design Process | 16 |
| 4.1 Needs Analysis | 16 |
| 4.2 Concept Mapping | 17 |
| 4.3 Alternative Designs | 17 |
| 4.4 Final Design Selection | 18 |
| Design Selection through Pugh Analysis | 18 |
| Final Design Concept Description | 19 |
| Initial Prototype | 19 |
| Final Prototype | 20 |
| Operational Mechanism | 22 |
| Chapter 5: Design Verification | 23 |
| 5.1 Decellularization | 23 |
| Initial Methodology | 23 |
| Initial Results | 23 |
| Secondary Methodology | 23 |
| Secondary Results | 24 |
| Final Methodology | 24 |

| | |
|---|----|
| Final Results | 25 |
| 5.2 Vacuum Chamber Design | 25 |
| 5.3 Dye Seeding Trials | 26 |
| 5.4 Sample Preparation | 27 |
| 5.5 Initial Cell Seeding Trial | 28 |
| Methodology | 28 |
| 5.5 Cell Proliferation Assay | 29 |
| 5.6 Initial Seeding Trials with Prototype | 30 |
| 5.7 Seeding Trial with Prototype - Higher Density | 31 |
| 5.8 Seeding Trial with Prototype - Final Trial | 31 |
| 5.9 Final Seeding Trial - Histological Results | 33 |
| Chapter 6: Final Design and Validation | 34 |
| Decellularization | 34 |
| Cell Seeding Device | 34 |
| 6.1 Economics | 34 |
| 6.2 Environmental Impact | 34 |
| 6.3 Societal Influence | 35 |
| 6.4 Political Ramifications | 35 |
| 6.5 Ethical Concerns | 35 |
| 6.6 Health and Safety Issues | 35 |
| 6.7 Manufacturability | 35 |
| 6.8 Sustainability | 36 |
| Chapter 7: Discussion | 37 |
| 7.1 Decellularization | 37 |
| 7.2 Device Design | 38 |
| 7.3 Cell Seeding | 39 |
| 7.3 Study Limitations | 39 |
| Chapter 8: Conclusions and Recommendations | 41 |
| References | 42 |
| Appendix A | 44 |
| Appendix B | 45 |
| Appendix C | 46 |

Authorship

This report is an accurate reflection of equal contributions from each of the team members. All team members contributed to the writing of this report, device design, and lab work for design and protocol testing.

Acknowledgements

We would like to thank Lisa Wall for taking the time and effort to help us obtain the needed materials for this project, as well as for helping with lab access and anything else we asked for. We would also like to acknowledge Jeffrey Huang, Dr. Erica Stults, Robert Kirch, and Ian Anderson in particular for help with printing and prototyping, and Marsha Rolle for helping us get a foundation of tissue engineering and for bouncing ideas off from. We would like to extend a very special thank you to Jyotsna Patel, who helped us with every step of this project, teaching us histology and showing us how to verify our results. Finally, we would like to thank our advisor, Sakthikumar Ambady, for coming up with this project and guiding us to its completion. It would not have been possible without you.

Abstract

Large volume tissue injuries, such as those in burn victims or myocardial infarction, have proven difficult to treat given the amount of tissue that must be replaced. One of the most promising forms of treatment is using a decellularized scaffold for the repopulation of autologous cells. Our approach shows proof of concept for the recellularization of thick scaffolds as for use *in vivo*. This project includes the development of a standardized decellularization procedure to create a scaffold out of a large volume tissue, the design of a microneedle device to seed cells onto a scaffold and verifies seeding and scaffold biocompatibility. Once developed further, this novel way of seeding cells onto large volume tissues could have major applications in wound healing.

Chapter 1: Introduction

Decellularized scaffolds are an approach being explored in the repair of large volume tissue injuries. The idea behind these scaffolds is to allow a patient's own cells to repopulate the scaffold after being applied to the injured area. However, our project focused on the repopulation of these scaffolds *prior* to their insertion into the body. In this way, the wound healing process would be facilitated and thus the injured area would heal much faster than other methods.

The recellularization of thick tissue scaffolds, however, remains a persistent challenge in developing adequate large volume tissue replacements as cells have difficulty penetrating further than the surface level. The seeding method we explored for our project was the use of microneedles in the delivery of target cells to the decellularized scaffold. We aimed to utilize microneedles in our device design to allow cells to be deposited and diffuse deeper in the scaffold with minimal damage to its structure.

Our project had two main goals. The first was to develop a decellularization procedure in order to create a scaffold to be used in the testing of our device. The second and more focused portion was to create a microneedle device capable of seeding live cells onto our decellularized scaffold.

Through this project a standardized decellularization procedure was developed. Once this was verified through histology, a syringe-based microneedle was designed. The decellularization protocol began with a standard detergent-based procedure in which we altered the time spent and concentrations of the reagents in each step to develop and standardize our process. In order to determine the efficacy of our results we have used histology and imaging to verify decellularization. Based on the designs we drafted, we initially 3D printed a microneedle array for our syringe-based prototype, but had to seek alternatives once we determined the capabilities for fabricating on this scale were limited. We developed a prototype that uses 25G hypodermic needles cut to a comparable solid microneedle length in a spring loaded array system. We also conducted a preliminary cell seeding trial to determine the biocompatibility of our scaffold as well as the depth and density of cell attachment using various seeding methods. We tested our device by injecting live cells into a decellularized scaffold with it and observing cell adherence, viability, and distribution throughout the full tissue depth.

In this paper we will discuss: (1) a literature review further diving into the issues this project addresses as well as prior solutions, (2) our project strategy further discussing our project goals and approach, and (3) our design process with other designs drafted, (4) the decision process to reach our final design, (5) the verification and validation methods for evaluating our device design and strategy, (6) the final design, (7) project outcomes and limitations and (8) conclusions and future recommendations.

Chapter 2: Literature Review

Tissue Engineering Background

Tissue Engineering is an interdisciplinary field that endeavors to create functional human tissues from isolated components with the goal of finding treatments and/or cures through the repairing, replacing, or regenerating of tissues or even organs that fail due to disease, genetic errors, congenital abnormalities, or traumatic injuries [1]. This is achieved through the manipulation of four key factors: cells, environment or scaffold, growth factors, and physical or mechanical forces. A popular approach is through the seeding of cells harvested from the target organ or developed from stem cells onto synthetic or natural scaffolds and promoting their growth and integration to mimic the target natural tissue's function [1]. Our project aims to improve upon the methodology of seeding target cells onto natural scaffolds, specifically in the reconstruction, replacement, and/or regeneration of thick tissues.

Although it is still considered an emerging field, as many advances are still to be made, the concept of tissue engineering has been around for a long time. One of the first accounts of rudimentary grafting was documented in 2500 B.C., in which gluteal fat and skin were used for cosmetic reconstruction of the ear, nose, and lip [2]. Today, the field of tissue engineering has expanded further than relocation. Currently, several tissues and whole organs have been successfully fabricated including, skin, cartilage, blood vessels, a bladder, and even the trachea. Although the field has seen immense growth, there are still many challenges to overcome in the creation of a completely vascularized, complex, functional organ, such as how to successfully seed cells onto thick tissue scaffolds.

Decellularization of Natural Tissue

Often for tissue engineering, natural tissue may be utilized for treatment. By decellularizing an existing tissue, an acellular scaffold with the ideal characteristics is achieved [3]. There are many methods of decellularization, each yielding different structural and mechanical property outcomes. Detergent-based treatments are common, and may use ionic, non-ionic, or zwitterionic/amphoteric solutions. SDS is the most common detergent used, but it may diminish desirable aspects of the matrix and biomolecules. Additionally, detergent-based methods have the potential to change growth properties and mechanical properties of the extracellular matrix [3].

Alternatively, enzymatic-based treatments may also be used to decellularize tissue. Enzymes target specific structures, and are used to remove antigenic material, decreasing the immunogenicity of the tissue. It is important that the enzymes be thoroughly washed when using this treatment however as remaining enzymes in the tissue can have adverse effects once in the patient. Enzymes such as nucleases specifically hydrolyze ribonucleotides, but can be difficult to remove and may cause an immune response. Trypsin specifically cleaves peptide bonds, but if not removed may damage the extracellular matrix (ECM) ultrastructure. Dispase cleaves specific peptides, but if not removed may damage important structural parts of the ECM [4]. This decellularization process is often used as supplements to detergents.

Finally, mechanical-based treatments may be utilized. Mechanical treatments include physical delamination, multiple freeze-thaw cycles, and high hydrostatic pressure [3], as well as supercritical fluid dissolution, pressure gradients, mechanical oscillations, sonication, and electroporation [4]. A study done by Sesli *et al.* [5] compares the effectiveness of detergent-based and freeze-and-thaw-based protocols in decellularizing adipose tissue, diaphragm, and heart and finds that a combination of SDS and Triton X-100 is efficient in providing porous and cyto-compatible scaffolds [5]. By combining a mix of decellularization methods, the preferred qualities of the tissue may be maintained, while still achieving a decellularized scaffold.

A Potential Application: Cardiac Grafts and Transplants

A potential application of decellularized tissues and scaffolds is in grafts for tissue and muscle injuries like that of myocardial infarction. Tissue-engineered myocardial grafts and organs are still largely in development as there are still several challenges to their large-scale manufacturing. Current therapies include various pharmacological (anticoagulants, ACE inhibitors, etc.), surgical, and catheter-based procedures that a physician will recommend based on the characterization of the heart attack [6].

In severe cases where there has been irreversible tissue damage, patients may undergo some form of tissue transplantation. A common surgical procedure for treating myocardial infarction is a coronary artery bypass graft (CABG) procedure in which the physician takes a length of vasculature from another area on the patient (typically the saphenous vein) to replace dead or blocked arteries in the heart [7]. This is an example of an autograft in which tissue is transplanted from one part of the body to another in the same individual. The advantages of this type of procedure is that there is no need for a compatible donor; however, it requires a second operation which can put patients at a greater risk of infection and is only possible for some treatments.

Another option for severe cases of myocardial infarction is a total organ transplant. This entails a patient receiving a heart from a donor which is implanted in place of the diseased organ. This treatment is an example of an allograft in which tissues are transplanted from a non-identical donor to a patient. While cardiac transplantation is an effective therapy in terms of restoring function, there are many risks with these procedures. Patients may suffer from lifelong immunosuppression and this procedure may never be available to all the patients in need because of the limited number of donors [8].

The heart's lack of regenerative capacity means that many of these treatment options, aside from full organ transplant, solely reduce symptoms or delay disease progress. There is still a need for treatment options that restore function to or replace cardiac muscle tissues. Our approach aims to restore function by replacing only the damaged tissue with a tissue scaffold that can integrate with the remaining muscle. The use of a decellularized scaffold for cardiac tissue treatments has been extensively explored as native tissue scaffolds maintain tissue specific microstructures and mechanical properties that can aid in recellularization and integration [9]. There are several challenges to this process in regards to cardiac tissues including balancing the

total decellularization of the scaffold sample while maintaining the necessary structural components, maintaining or promoting vascularization, and achieving even dispersion and adherence of target cells to the full depth of the tissue [9].

Microneedles

Microneedles are extremely small needles used in a variety of functions and are created in many different form factors. The four most commonly used forms of microneedles are solid, coated, hollow, and dissolvable. The differences between the four categories could be demonstrated by the example of a drug treatment in the form of a liquid trying to bypass the skin layer. Solid microneedles are largely used as pre-treatment devices. They would create tiny holes in the skin to which the treatment is then applied. Coated microneedles are solid microneedles coated with the drug that help facilitate the delivery process when the needle penetrates the skin. In hollow microneedles, the drug would be loaded into the microneedle and then dispensed from the needle following penetration. The dispersion process is most commonly carried out through diffusion out of the hollow needle or by applying a force to push the treatment out. Lastly there are dissolvable microneedles made entirely of the drug. After being applied to the skin, the needles would stay there until they eventually dissolved [10].

Microneedles have a variety of uses and are still growing as their capabilities are further explored. To begin, microneedles are often studied in their capabilities to be used as a transdermal drug delivery system for disease treatments. They serve as a potential alternative to hypodermic needles which are much larger and much more painful for patients. Two studies discussed by Yang *et al.* [10] are in the treatment of cancer and diabetes. Researchers looked into a way to deliver chemotherapeutic drugs to cancer patients using dissolving microneedles. On the diabetes side, scientists tested the capabilities of a smart insulin patch using a microneedle array that would detect and respond to fluctuating glucose levels in patients accordingly. Other applications of microneedles discussed in this article were in disease diagnosis and cosmetics.

Using hollow microneedles, a team of researchers withdrew skin interstitial fluid from patients to analyze the metabolites present. In this way they were able to diagnose diseases such as diabetes using microneedle arrays. Cosmetics are a more commercial application of microneedles. Pimple patches are typically composed of coated or hollow microneedles that are loaded with acne medication to be placed on skin in need of treatment and left on for a time before the drug has had ample time to transfer. Microneedle rollers are another form of cosmetic treatment used commercially. These rollers pierce the skin to trigger the wound healing process in users [10].

The fabrication of microneedles can be assessed based on its uniformity and reproducibility of the specified needle geometries which can be difficult to achieve on a small scale. The most common method of fabrication is through the use of lithography-based molding methods in which a pattern is etched out of a substance often via laser [11]. These processes, however, are not only time consuming but require specialized equipment, facilities, and training which make it less accessible. In recent years, as 3D printing capabilities have expanded, this

method of microneedle fabrication has begun to present a promising approach for a more cost-effective approach with a quicker turnaround time. 3D printing also allows for greater freedom of customization regarding size and material [12].

Prior Arts: Gold Standard: Clemson Study

In a project done at Clemson University, microneedle arrays were used to deliver cells into decellularized carotid arteries and aortic cups. The researchers used several different microneedle arrays to be tested in this application. These microneedle arrays were used to inject cells into the decellularized carotid arteries and aortic cusps. The researchers found that while these arrays succeeded in seeding cells on the aortic cusps, there was difficulty in seeding the cells on the carotid arteries. The results of the study showed that there were difficulties in using the microneedles to inject into dense tissues but that the microneedle design could be adjusted to better tailor it to a specific tissue. The prototype device developed in this study serves as our gold standard as it demonstrated capabilities of seeding cells onto a decellularized scaffold using microneedles. The researchers had difficulty seeding cells into a tissue that was 2 cm thick [13]. Our goals are to be able to use a microneedle device to seed cells on tissue at least 1cm thick with a cell density similar to that of native muscle tissue [14]. As such, this study shows us a previously existing device to improve upon and apply to our situation.

Prior Arts: Cell Seeding Techniques

Looking at previous cell seeding techniques allows for design comparisons and incorporations into our project's cell delivery system. Villanova *et al.* [15] provides a summary and comparison of current available techniques. The most common method of cell delivery is passive seeding also known as static or gravitational seeding. This technique is based upon the direct pipetting of the cell suspension into the lumen or outside the scaffold. Static seeding is the most ineffective method discussed, with cell seeding efficiency of only 10-25%. While the method is simple, static seeding comes with multiple disadvantages including inconsistency and operator dependence. Another seeding technique discussed is rotational and centrifugal systems where the scaffold is spun within the cell suspension in conditions about 0.2-500 rpm. The method has substantially increased seeding efficiency and scaffold penetration, although speed and its effect on cell morphology are considered possible drawbacks of rotational and centrifugal systems. Vacuum seeding technique is a system that relies upon the pressure differences to see cells into the scaffold. The method is simple, rapid, with high seeding efficiency that our project could consider for the delivery design. Other techniques including magnetic and electrostatic systems, despite showing higher seeding efficiency, include risks such as adverse or unknown long-term effects on cell proliferation [15].

In order for successful cell seeding to occur, there are several factors that must be considered. Factors for successful seeding include cell type, cell number, seeding strategies, and the culture system characteristics [16]. In terms of cell type, parenchymal cells or nonparenchymal cells can be used. Parenchymal cells used to seed muscle tissue may be

myocytes, while nonparenchymal cells may include endothelial cells as a nonthrombogenic barrier, or fibroblasts to secrete and remodel the ECM. Cell number is dependent upon which type of tissue is being reseeded, and the cells can either be seeded as a small number of proliferative cells, a large number of fully mature cells, or a mix of these two. Seeding strategies, which were previously discussed, usually are either intramural injection of cells, meaning the cells are directly inserted into the organ, or through continuous perfusion, which involves a constant exchange of media and cells [16]. Finally, culture system characteristics are important for cell survival. For instance, there must be a delivery of nutrients into the scaffold, and harmful waste products need to be removed. *In vitro*, this is usually done through perfusion in a bioreactor. Perfusion requires a suitable perfusion medium, an oxygen carrier, and, based on tissue type, a biophysical simulation. The perfusion medium, or perfusate, is dependent on cell type, and the oxygen delivery can be achieved through gassing the perfusate mixture. For example, gassing the perfusate with 95% oxygen and 5% carbon dioxide will lead to a partial pressure of oxygen of 360 mmHg, which is sufficient for the demand of cardiomyocyte cells, which requires metabolic demand of oxygen equaling 27.6 nmol/mg per minute [16]. Together, these techniques may vary based on tissue type, but can yield a recellularized scaffold.

Chapter 3: Project Strategy

3.1 Initial Client Statement

Use of decellularized scaffolds is a promising approach to repairing large volume muscle injuries and burn injuries. There are two options for using decellularized tissue scaffolds: (a) transplant a decellularized patch to the injured area to allow native cells to migrate and repopulate the patch or (b) repopulate the patch with cells in vitro prior to transplantation. One of the biggest challenges to the latter approach is the inability to efficiently repopulate cells to deeper regions of decellularized tissue patches.

The goal of this project is to design microneedles or nanoneedles to deliver live cells into decellularized tissue patches. In this project we aim to:

1. Develop a method to produce micro/nano needle cell injection device capable of delivering precise volumes of a cell suspension into varying depths of 1 to 5 cm thick decellularized patches.
2. Standardize procedure(s) to decellularize tissue patches and quantitatively demonstrate efficiency of decellularization.
3. Use quantitative approaches to demonstrate that micro injected cells are able to survive, proliferate, and populate the decellularized tissue patch over a period of days to weeks as applicable.

3.2 Design Requirements (Technical)

For the scope of this project, technical design requirements of the microneedle device can be broken down into functional and performance specifications. In terms of functions of the device, a system needs to be created that penetrates the tissue surface, dispenses cells, disperses cells evenly, and adheres them to the decellularized scaffold. Additionally, cell viability must be maintained, so that cells proliferate and thus populate the scaffold. For performance specifications, cells must be seeded at a minimum of 1 cm, dispersed at a density of 1.0×10^8 cells per cm^3 , and an adherence of approximately 90% to the scaffold should be achieved. Additionally, the concentration of cells should be kept at approximately $5 \times 10^5/\text{cm}^3$, with green fluorescence protein used to verify cell seeding [14].

3.3 Design Requirements (Standards)

In order to ensure the microneedle function, a final device must follow the ISO D695 standard for compression testing protocol, ensuring the needle will not break under pressure. Additionally, tensile testing should be done following the American Society for Testing and Materials (ASTM) D822 standard for determining tensile properties [17]. As the end product is a tissue engineered scaffold, a cell potency assay should also be run following the ASTM F3368-19 standard for tissue engineered products [18]. Finally, this device should follow the International Electrochemical Commission's standard for sustainable medical devices (IEC 60601-9). This ensures that the device is safe, and effective [19].

In terms of the decellularized scaffold, the developed protocol must follow ASTM F3354-19, the standard for evaluating extracellular matrix decellularization processes [20]. While this standard indicates that there is no determined consensus for decellularization thresholds, ideally, one specific evaluation method within this is a lack of nuclear material when visualized with DAPI staining. This is important as removal of nuclear material ensures that decellularized material is safe. Additionally, the ISO 10993 standard should be considered for biocompatibility [20], to ensure that living material can survive on the scaffold.

3.4 Revised Client Statement

The goal of our project is to design a microneedle delivery system capable of seeding cells into thick decellularized tissues and maintaining cell viability for regenerative therapy in clients with large volume tissue injuries. First, a procedure must be developed to decellularize tissue which must be validated with no nuclei present as indicated through histology. Second, the delivery system must be able to seed cells into at least a one centimeter scaffold tissue. The design needs to have cell efficiency and viability after delivery of about 90%. Specific microneedle and cell delivery specifications [14] include:

1. Penetrate tissue to a depth of at least 1cm and adequately deliver cells
2. Maintain a concentration of approximately 5×10^5 cells/cm³;
3. Achieve approximately 90% adherence of cells to scaffold;
4. Disperse cells at a density of 1.0×10^8 /cm³;
5. Verify cell seeding with fluorescence over time;

3.5 Management Approach

This project was broken down into three main components: decellularization, device design and fabrication, and verification and validation. By splitting the project into these steps, we have more realistic steps towards achieving the goal of a reseeded decellularized scaffold. This project spans the timeline of August, 2021 to May, 2022 (with expected commencement of May 14th). The project started in the fall semester, particularly with decellularization. Device design and fabrication then occurred as histological verification of decellularized samples was underway. Once the device was fabricated and functional, device validation and verification occurred, putting the timeline near the end of the second semester. The in-depth breakdown of our work schedule can be seen visually in the Gantt chart in Figure 1.



Figure 1: Gantt Chart Work Breakdown

Chapter 4: Design Process

4.1 Needs Analysis

The first step of this project was to create a decellularization procedure that would fully remove nuclear material from a tissue, leaving only a functional scaffold. This was imperative as it mimics biological tissue scaffolds that would be used in the future of this device. For potential treatment applications, remaining nuclear material in a decellularized scaffold can result in immune rejection, making this step essential. For our microneedle system there were three specific needs that needed to be met. The first was that our design needed to penetrate the scaffold to create a place for the cells to enter. Secondly, the microneedle system needed to dispense cells into the scaffold. Lastly, the system should be able to disperse and distribute the cells evenly throughout the scaffold. This ensures they are physiologically as close to native tissue as possible.

In order to help in the process, the design of a microneedle system was further broken into five design criteria. These were determined to be penetrating the scaffold, adhering cells to the scaffold, dispersing cells, dispensing cells, and maintaining cell viability. These were then ranked through pairwise comparison, as shown in Table 1. Each criterium was ranked as less important than (0), equally important as (0.5) or more important than (1) the other criteria. This revealed the mechanism of cell dispersion to be the most important factor, followed closely by the mechanism to penetrate the scaffold, and then adhere the cells to the scaffold. Dispersing the cells and maintaining cell viability were ranked as comparatively less important, as this project seeks to show proof of concept of a cell delivery method for deep tissue scaffolds.

Table 1: Pairwise comparison chart for design criteria rankings

| | Penetrate Scaffold | Adhere Cells to Scaffold | Disperse Cells | Dispense Cells | Maintain Cell Viability | Total |
|--------------------------|--------------------|--------------------------|----------------|----------------|-------------------------|-------|
| Penetrate Scaffold | | 1 | 1 | 0 | 1 | 3 |
| Adhere Cells to Scaffold | 0 | | 1 | 0 | 1 | 2 |
| Disperse Cells | 0 | 0 | | 0 | 0.5 | 0.5 |
| Dispense Cells | 1 | 1 | 1 | | 1 | 4 |
| Maintain Cell Viability | 0 | 0 | 0.5 | 0 | | 0.5 |

4.2 Concept Mapping

In the concept map seen in Figure 2, our goal was initially broken down into its three main subsections: decellularizing the tissue, penetrating the tissue, and seeding cells onto the tissue. These were further broken down into additional methods of accomplishing the initial goal. From this, we determined that decellularization could be done with either a freezing or a detergent-based methodology. Once completed, the procedure will be evaluated with histology and revised, if needed. In order to penetrate the tissue, the team will utilize a microneedle, as given by the client statement. Types of microneedles include solid, coated, dissolving, and hollow microneedles, some of which are the injection mechanism for the cells. Finally, to make a cell suspension, cells could be present either on the microneedle or inside the microneedle, and media is required to proliferate the cells.

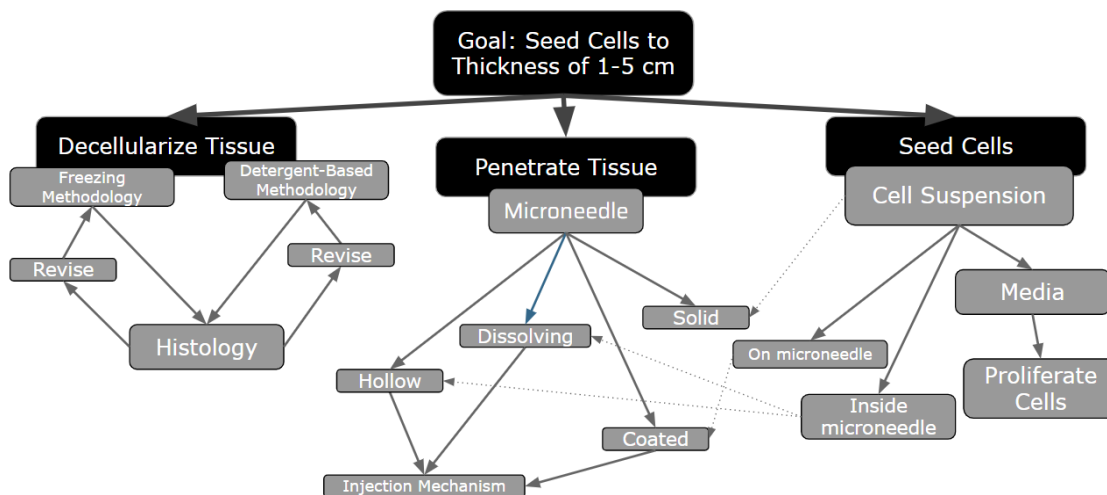


Figure 2: Concept map of design options

4.3 Alternative Designs

Based on the specifications highlighted in our needs statement, our team brainstormed ways to answer the following questions: How do we deliver cells to the scaffold? How will the scaffold be penetrated? How will cells be seeded? The resulting designs incorporate a mechanism or feature that addresses each of these concerns. Our team came up with five initial microneedle designs (as seen as Figures 3 and 4).

Our first design was a dissolving microneedle array. For this, the cells would be encapsulated in a biodegradable compound (e.g. hydro-gel) and be formed into the microneedles themselves. Once they penetrate the scaffold the needles would then dissolve to release the cells into the scaffold as shown in Figure 2. Our second design was a solid microneedle array and a vacuum pump. For this design, we drew inspiration from traditional microneedle designs like those used for derma rollers. The roller would be used to penetrate the scaffold and create micropores that the cell solution could seep into once dispensed on top. Because this design has no mechanism to encourage seeding cells into the tissue, a vacuum treatment is a necessary part

of the design to draw the solution into the scaffold as shown in Figure 2. The microneedle device would not be sufficient on its own. Our third design utilizes magnetic force to deliver cells to the scaffold. This process would first require that the target cells be treated with ferrous particles so they can be directed via a magnet. The microneedles would be made to have a charge and function as electrodes with which to direct the dispersion of the cells as shown in Figure 2. The fourth design focuses on hollow microneedles. The cell solution would be drawn up into the microneedles which would penetrate the scaffold and a syringe style pump would apply the force to dispense the cells through the scaffold as shown in Figure 3. This design addresses all the features of our guiding questions in one device. The limitations of this design are due to the fact that the needle depth may not be sufficient with just a microneedle. The fifth design involves the use of solid microneedles coated in the target cell population. The microneedle array, with the cells adhered, would be pressed into the tissue, and penetrate the scaffold to deposit the cells where it contacts the tissue as shown in Figure 3. This method would also have no additional force applied and could potentially be used in conjunction with the vacuum apparatus to improve depth of seeding.

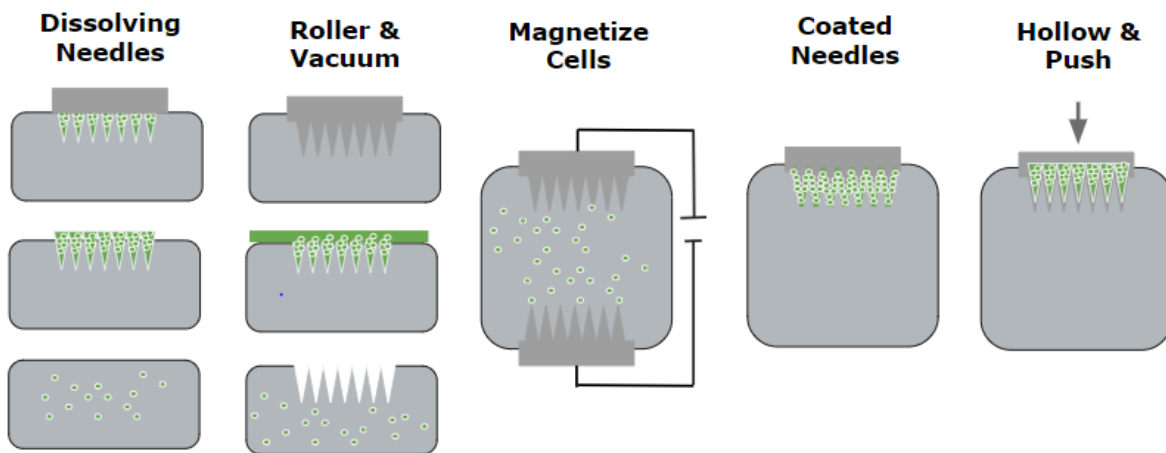


Figure 3: Initial Design Concepts

4.4 Final Design Selection

Design Selection through Pugh Analysis

Having rated the specs through the pairwise comparison chart (see chapter 4.1), the designs were assigned weights based on their rankings (shown in Table 2). With no established gold standard for cell seeding into decellularized tissue, the microneedle array from the Clemson University study was chosen as a gold standard. Based on ranking against the gold standard, the dissolving microneedles were found to perform at the baseline. Design 2, the roller and vacuum method, we believe would perform worse than the baseline. Design 3, the magnetization of cells, was rated at the same level as the baseline. Design 4, the hollow microneedles is designed to penetrate thicker tissue with a syringe-like mechanism to push the cells out. We would tailor it to penetrate the scaffold in a much more effective way than the current standard. As such, this

design was ranked above the baseline (+4, Running Total = 4). Finally, Design 5 - the coated microneedle, we believe would perform worse than the baseline).

Having evaluated all of the concepts, Design 4 - the hollow microneedles was selected as optimal. It will be designed to penetrate thicker tissue, with a syringe-like mechanism to push cells out. It was therefore determined to have the highest score, and thus was selected as the final design through the Pugh analysis.

Table 2: Pugh analysis for final design selection

| Criteria | Weight | Standard: Clemson Study | Dissolving Needles | Roller and Vacuum | Magnetized Cells | Coated Needles | Hollow and Push |
|--------------------------|--------|-------------------------|--------------------|-------------------|------------------|----------------|-----------------|
| Penetrate Scaffold | 4 | 0 | 0 | 0 | 0 | 0 | 1 |
| Adhere Cells to Scaffold | 3 | 0 | 0 | -1 | 0 | 0 | 0 |
| Disperse Cells | 1 | 0 | 1 | 1 | 1 | 0 | 0 |
| Dispense Cells | 5 | 0 | 0 | 0 | 0 | 0 | 0 |
| Maintain Cell Viability | 1 | 0 | -1 | 1 | -1 | -1 | 0 |
| Total | | 0 | 0 | -2 | 0 | -1 | 4 |

Final Design Concept Description

The main reasoning behind the hollow microneedles design is the fact that it is based upon the successful gold standard of a smaller scale. In this previous study done by Clemson University [13], the hollow microneedles design showed promising results of penetrating and seeding cells into tissues of thickness 3-6 mm. This result provides a significant theoretical and practical foundation for our consideration of the design for thicker tissue applications. The implementation of this concept in our project is then to test its effectiveness and limits when working with deeper tissues. Some design parameters our project considered changing were depth, width, and thickness of the needle walls. As a result, the hollow microneedles concept for our project's goal is testing the scalability of this previous successful design. Additionally, this design required a final procedure for cell seeding with the microneedle.

Initial Prototype

To make a functioning hollow and push microneedle array, initially a microneedle with specifications similar to those of the Clemson study was designed. In Figure 4, the microneedle array was designed to test the resolution of the 3D printer, having a 0.5 mm height, 0.06 mm minimum outer diameter, and 0.05 minimum inner diameter. This device was designed to attach to a syringe and was printed. While the connection to the Luer-lock syringe was functional, the

print along with subsequent resolution printing tests confirmed that the Form2 printer lacked the resolution to create hollow tips smaller than 1 mm. Therefore, what resulted was a dull solid microneedle, shown in Figure 5. Therefore, the Form2 printer was not sufficient for printing a hollow microneedle. Fortunately, this prototype showed that attachment to the Luer-lock syringe was a feasible design choice.

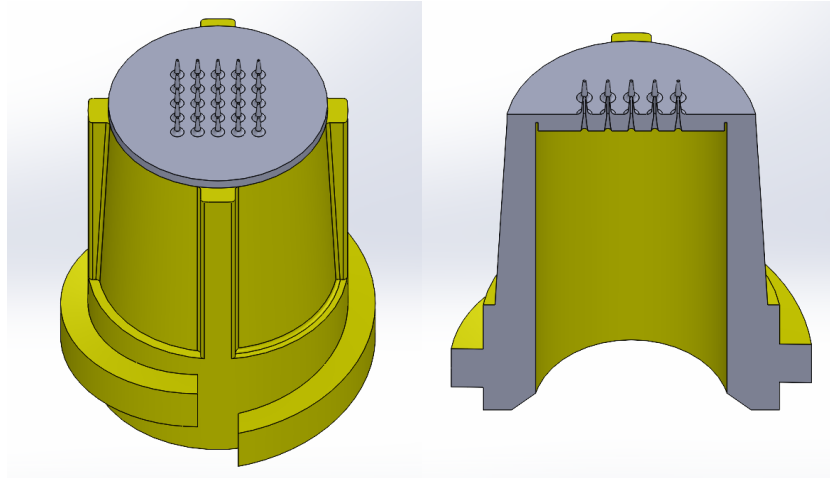


Figure 4: CAD of initial hollow microneedle array. See Appendix B for the detailed dimensions of the design.



Figure 5: The prototype of the previous iteration of the hollow microneedle array

Final Prototype

The limitation of 3D printing resolution and the tissue penetration depth of 1 cm inspired us to design the needle component around pre-existing hypodermic needles of the desired dimension ranges, as illustrated in Table 3.

Table 3: Some considered standard gauges for hypodermic needles within the desirable dimension ranges

| Needle Gauge | Outer Diameter | Inner Diameter | Wall Thickness | Length Available |
|--------------|--------------------------|-------------------------|------------------------|---|
| 25G | 0.5144 mm/ 0.02025 in | 0.260 mm/ 0.01025 in | 0.1270 mm/ 0.005 in | 15.875 mm ($\frac{5}{8}$ in), 25.4 mm (1 in), 38.09 mm (1½ in) |
| 27G | 0.4128 mm/ 0.01625 in | 0.210 mm/ 0.00825 in | 0.1016 mm/ 0.004 in | 12.7 mm ($\frac{1}{2}$ in), 31.75 mm (1¼ in) |
| 30G | 0.3112 mm/ 0.01225 in | 0.159 mm/ 0.00625 in | 0.0762 mm/ 0.003 in | 12.7 mm ($\frac{1}{2}$ in), 25.4 mm (1 in) |

The final device has an interior reservoir of the syringes, allowing them to hold cells. These will be able to pierce the tissue and inject cells inside the sample. In order to complete this, a syringe, or “pushing” mechanism forces the cells out of the syringe. The Luer-lock design was chosen for our syringe adapter component so that the design could be adapted to most commercially available standard syringes to measure the volume of cell suspension to be recellularized.

The challenge of needles bending during injection due to high length to diameter needle ratio and large number of needles were also considered. As a result, the double concentric platform system was implemented to hold the needles straight and account for any lateral movements from tissue penetration. The spring component serves primarily as the retractable mechanism after injecting the cells into the scaffold and secondary as a spacer between platforms and protection from open needles. A threaded cap is designed to protect the user from potentially exposed needles.

In general, our final microneedle prototype comprises the four components functioning as elaborated above. Specifically, Figure 6 demonstrates a version of the final design with 7 25.4 mm-long 25G needles with springs that would expose about 1 cm of needles when fully compressed into our 1 cm tissue samples. However, the more general design accounts for variability in number, type, and length of both the needle and spring components as well as the area and patterns of needles for different scaffold sizes. The design could then be optimized for different applications by modifying these parameters.

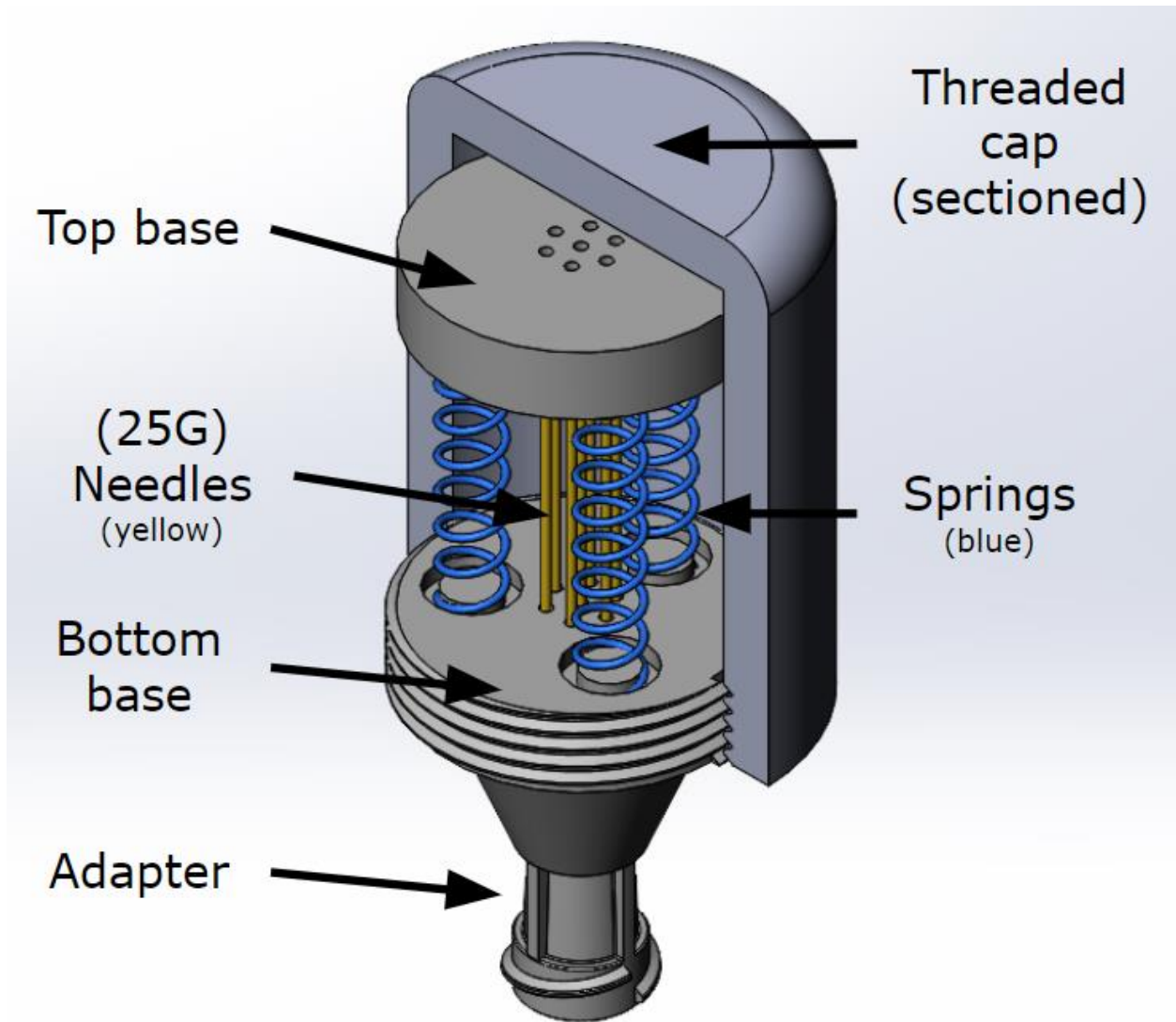


Figure 6: Final design of the microneedle delivery system with cross-sectioned threaded cap. See Appendix C for detailed dimensions of the full device and its components.

Operational Mechanism

From the design, our team developed a protocol on how to use our device in a syringe system to seed cells into the decellularized tissue. After the syringe is loaded with the desired cell suspension, the device could adapt to the syringe using the Luer-lock mechanism. The whole syringe should be used to fully compress the springs and expose the needles into the tissue. The plunger flange would then be held in place while letting the barrel naturally come up from the springs' retractable force, dispensing the cell suspension into the tissue through the motion.

Chapter 5: Design Verification

5.1 Decellularization

Initial Methodology

Using the outlines of an existing protocol published by Sesli *et al.* [5], a protocol for cell seeding was devised utilizing SDS and Triton X-100. The purpose of this initial experiment was to evaluate the effectiveness of the standard protocol against varying concentrations of reagents, time periods, and conditions.

The standard protocol was followed for three samples of chicken of approximately 1 cm by 1 cm in cross-sectional area. They were rotated vertically at 100 rpm for two days in 0.5% SDS. They were then washed with PBS and rotated in approximately 15 mL of 1% SDS for one day. They were then rinsed with PBS again and rotated in approximately 15 mL of Triton X-100 for one hour. The samples were then rinsed with PBS and stored in PBS/PennStrep in the fridge.

This protocol was then varied in four additional ways, each testing a different condition. The first variation used three samples and doubled the SDS concentration in each step with SDS. The second variation of three samples doubled the Triton-X concentration, making it 2%. The third variation doubled the time for three samples, and the final variation used a vacuum between each step to remove all air which may be inside the sample and liquid.

Initial Results

Histology was done on the exterior of each of the samples, and upon analysis under a confocal microscope, successful decellularization was confirmed by a lack of nuclei. No notable difference was seen visually between the samples.

Secondary Methodology

The purpose of this experiment was to standardize a decellularization protocol given the results of Decellularization Experiment 1. In particular, we wanted to remove the ambiguity of amounts of reagents, and rinse times. For this experiment, we used a ratio of 3mL reagents per gram of sample, and standardized the rinse times to 10 minutes. We also removed the rinse between SDS solutions, as the same reagent was being used.

For the final protocol, three raw chicken breast samples were prepared with a cross-sectional area of approximately 1 cm². Masses were taken of each sample prior to placing them in a numbered 50 mL conical vial. 3 mL of 0.5% SDS per gram of chicken were then added to each tube. The conical tubes were sealed with parafilm, then placed onto the Rotomini (24 rpm) for 48 hours. After 48 hours, the 0.5% SDS was replaced with 1% SDS. The tubes were again sealed with parafilm and placed back onto the Rotomini for 24 hours. After 24 hours, the SDS was aspirated and 3 mL/g Dulbecco's Phosphate Buffered Saline without Ca⁺⁺/Mg⁺⁺ (DPBS-) was used to rinse the samples, placing them back on the Rotomini for 10 minutes. Once rinsed, 3 mL/g of 1% Triton X-100 was placed into each tube. The tubes were sealed and rotated for another hour. After an hour, the Triton X-100 was aspirated and another rinse of DPBS- was

done in the same way. Finally, the samples were stored in the fridge in a DPBS/PennStrep solution.

Secondary Results

Histological analysis of these samples was conducted on both the exterior and interior of the sample. Viewing of exterior samples under a confocal microscope showed that minimal to no nuclear material remained in the sample. However, interior samples showed blue remnants of nuclear material. While no nuclei remained, meaning the cells had been destroyed, the blue nuclear material indicated that not all the DNA was successfully removed, as seen below.

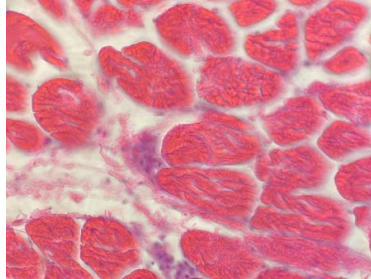


Figure 7: Decellularized sample with no nuclei, but remaining nuclear material (blue)

Final Methodology

As there was presence of nuclear material remaining, a series of three 10 minute DPBS washes was evaluated alongside a series of 6 washes at 10 minute per wash. Histological analysis showed no difference between nuclear material presence in the two, so the three washes were determined to be the more efficient.

The following protocol was therefore used for sample preparation:

1. Prepare samples to a cross sectional area of 1 cm x 1 cm.
2. Take the mass of each sample.
3. Place each sample into a 50 mL conical tube.
4. Add 3mL/g of 0.5% SDS into each tube, and seal with parafilm.
5. Place the tubes onto the rotomini to spin at 24 rpm for 48 hours.
6. Remove the samples and aspirate the SDS.
7. Add 3mL/g 1% of SDS to the tubes. Seal with parafilm.
8. Place back on the rotomini for 24 hours.
9. Aspirate the SDS.
10. Wash samples with 3mL/g of DPBS- for 10 minutes on the rotomini.
11. Aspirate the DPBS-.
12. Add 3mL/g of 1% Triton X-100. Seal with parafilm and return to the rotomini for one hour.
13. Aspirate the Triton X-100.
14. Repeat steps 10 and 11 three times.
15. Store samples in the fridge (4°C) in 3mL/g of PBS/1% PennStrep. Use DPBS+ if cell seeding is intended for the samples.

Final Results

After sectioning and staining the samples, histological analysis on the interior and exterior slices of the samples showed no nuclei, and minimal remaining nuclear material. Therefore, it was concluded that there was no difference between the three and six washes in terms of nucleic material presence. This can be seen in the images below. All samples appeared similar to the ones shown.

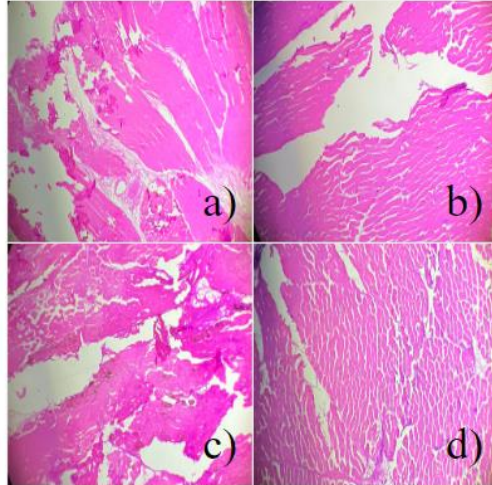


Figure 8: Final decellularization results taken at 40X magnification. a and b represent the exterior and interior of the sample with three washes, respectively. c and d represent the exterior and interior of the samples with six washes, respectively.

5.2 Vacuum Chamber Design

To further test seeding mechanisms, a vacuum chamber with one way flow was designed. It was created by cutting a hole into an existing tupperware container and creating a nozzle for the vacuum to attach. Then, a bottom plate and top plate were designed to create unidirectional flow, so when a sample was placed on top, there would be negative force downward. Finally, the chamber was sealed with parafilm around the lid prior to using the vacuum. The chamber functions to draw a cell suspension through the vacuum, allowing a different mechanism of seeding to be evaluated. However, after preliminary trials with samples, we found that the unidirectional flow was not narrow enough around the sample, and therefore the device was not used in future trials. The final device is shown in Figure 9.

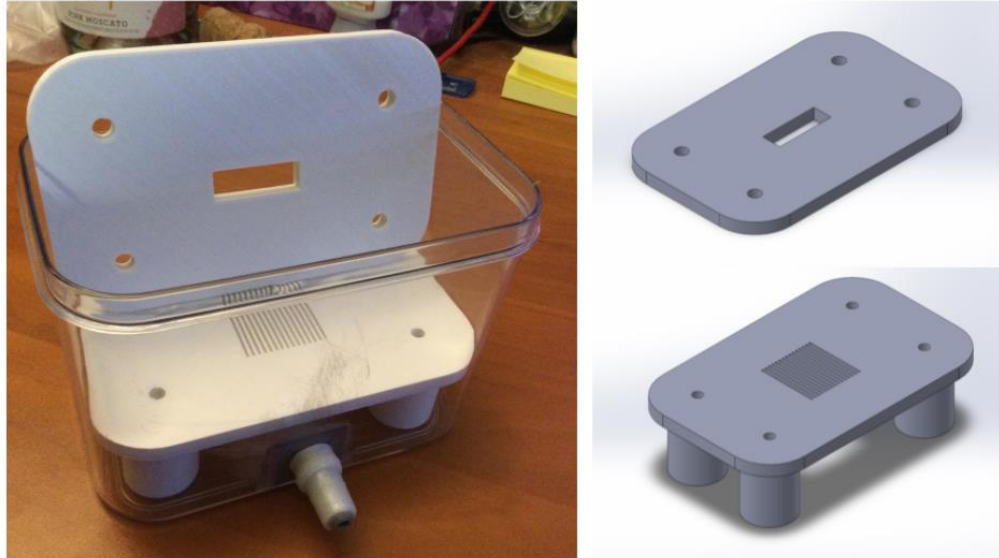


Figure 9: Vacuum chamber design and final prototype

5.3 Dye Seeding Trials

Dye seeding trials were conducted in an attempt to visualize possible results of seeding trials using different methods. The derma roller, topical, 30G needle, vacuum, and submerged methods were all tested. All conditions were run in triplicate.

The derma roller's needles were coated in food dye and rolled across the surface of a 1 cm chicken slice. In the topical method, 25uL of food dye was pipetted onto the surface of a 1 cm chicken slice. The 30G needle was inserted into the center of the 1 cm chicken slice. Tape was used to mark 1mm on the needle as this was the depth the needle was pushed into and where the 25uL of dye was dispensed. The vacuum method entailed adding 25uL of the food coloring dye topically and then adding the chicken slice into the vacuum chamber for either 5, 8, or 10 minutes. In the submerged method, the 1cm chicken slice was added to a well plate which was flooded with 2mL of food dye. Each of the three pieces was removed at 30, 45, or 60 minutes respectively.

The most promising of the seeding methods based on this preliminary analysis was the submerged condition, as seen in the figure below.

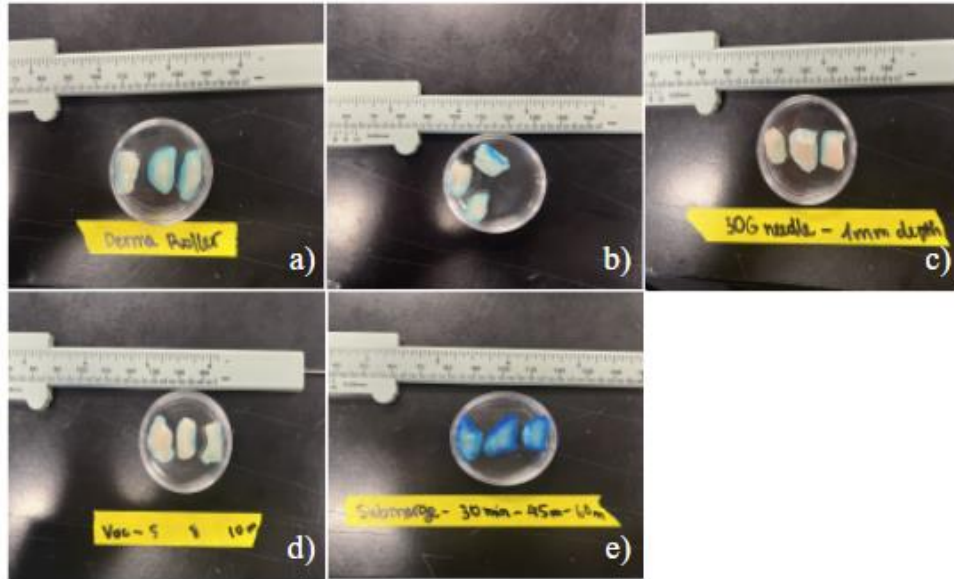


Figure 10: Results of dye seeding trials. a) derma roller; b) topical; c) 30G needle; d) vacuum and e) submerged.

To verify the seeding depth of our device to be 1 cm, India ink was loaded onto a 1 mL syringe with our needle device. A 1x1 cm sample strip of decellularized tissue was prepared beforehand and the device was used to dispense the ink along the sample's long axis. The tissue was then cross sectioned as shown in Figure 11 to visualize the depth of our seeding device, which confirmed that our device could reach about 1 cm into the tissue. The black ink seen on the outer surface of the tissue is due to overflown ink from the seeding process.

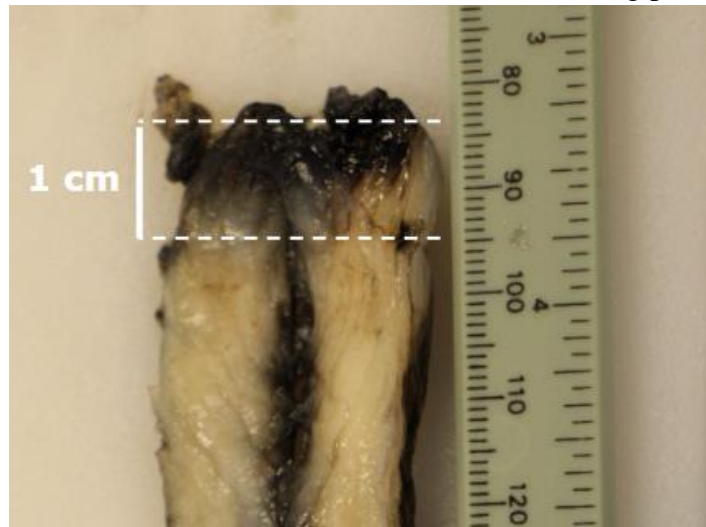


Figure 11: Result of India ink seeding depth trials

5.4 Sample Preparation

To prepare samples for cell seeding, the final standardized decellularization protocol was utilized. Once prepared, samples were cut to the ideal size for seeding, then sterilized in 70%

ethanol for 2 hours. They were then washed in DPBS+ three times for approximately 1 minute to dilute out the remaining ethanol. Finally, they were placed in the incubator in complete medium overnight, prior to usage.

5.5 Initial Cell Seeding Trial

Methodology

Once dye seeding was done, cell seeding was then done with the same methods using MDA-MB-231-GFP cells. Cells were seeded onto 1 cm³ decellularized chicken samples. The derma roller was rolled over the top of the scaffold twice, then cells were seeded on top (800k cells in 50 μ L complete medium). For static seeding, 800k cells in 50 μ L complete medium were placed on top of the scaffold. For the hypodermic needle, 800k cells in 1 mL of complete medium were injected into 5 locations of the scaffold with a 30G needle. For the vacuum, static seeding was repeated, then the vacuum chamber was run for 3 pulses of 10 seconds. These samples were left for 1 hour to allow them to adhere to the scaffold, then flooded with approximately 2.5 mL of complete medium. Finally, samples were submerged in 2.5 mL of complete medium with 800k cells. Each of these was run in triplicate. Complete medium was changed every 3-4 days, for a total of two weeks.

Biocompatibility Results

To ensure biocompatibility of the scaffold and ensure proper cell seeding, the cells were viewed under an inverted fluorescence microscope. The cells fluoresce green in the static and submerged samples, while the other samples were likely seeded deeper, not permitting surface visualization. The cells seeded in the topic seeding appeared dense, likely indicating too high a seeding density, but overall showed scaffold compatibility. The submerged samples further supported that the decellularized samples were biocompatible, and showed elongated structures, indicating that the cells were able to proliferate. These are shown below, with images taken two days after seeding.

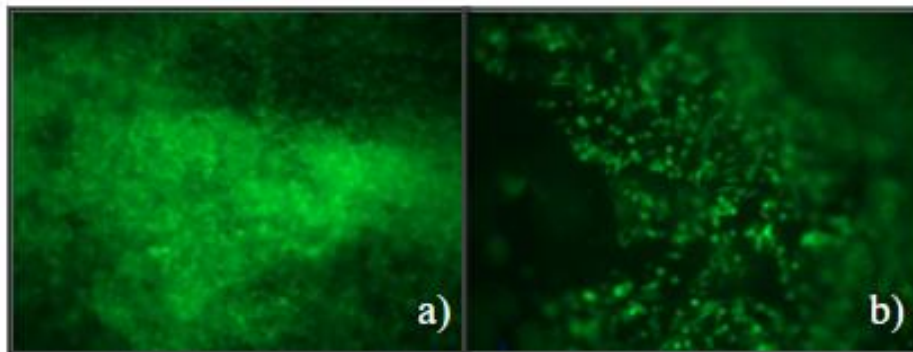


Figure 12: a) Static Seeding of 800k cells; b) Submerged seeding of 800k cells

5.5 Cell Proliferation Assay

To visualize the rate of cell proliferation, a BrdU assay was run to evaluate the difference between proliferation on the decellularized samples compared to cell culture plastic. Two 0.25 cm thick samples were prepared and seeded with 50k cells. The results showed cell division on both cell culture plastic and the tissue samples. These are shown in Figures 13, with the nuclear material in blue and nuclear material of proliferating cells in red.

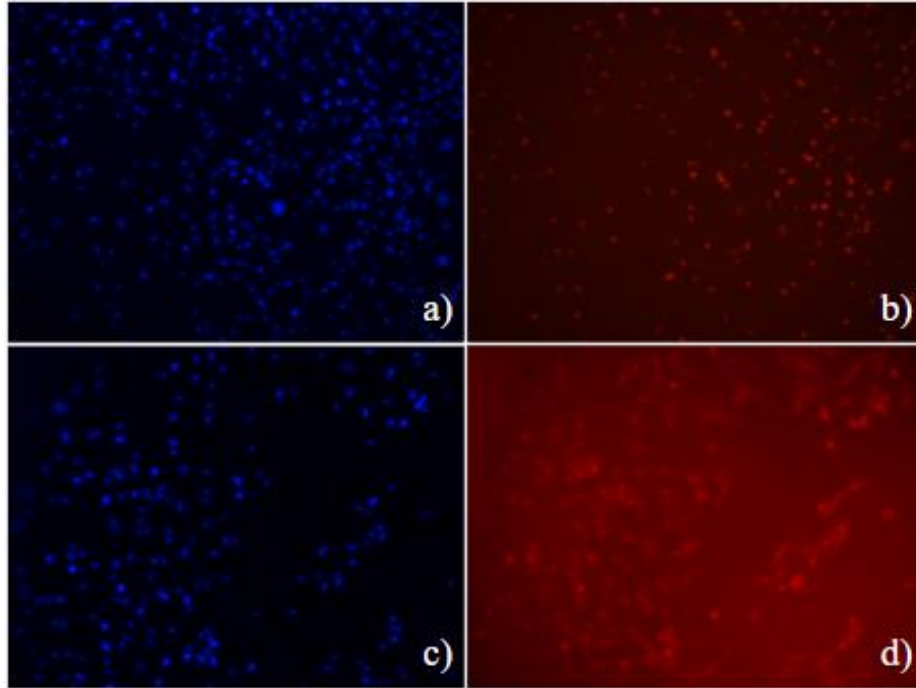


Figure 13: a) DAPI MDA-MB-231-GFP cells BrdU assay on culture plastic; b) BrdU MDA-MB-231-GFP cells BrdU assay on culture plastic; c) DAPI MDA-MB-231-GFP cells BrdU assay on tissue sample; d) BrdU MDA-MB-231-GFP cells BrdU assay on tissue sample

ImageJ was used to analyze the cell culture plastic images. Specifically, the images were converted into 8-bit images. They were then thresholded to obtain a black and white image. A watershed was applied to separate adjacent nuclei. Finally, the “analyze particles” feature was used to get a total count of nuclei. For cell culture plastic, there were 462 cells, with 277 dividing cells. From the equation below, the proliferation rate of MDA-MB-231-GFP cells on cell culture plastic was determined to be approximately 60%.

$$\frac{277 \text{ dividing cells}}{462 \text{ cells}} * 100\% = 0.60 * 100\% = 60\%$$

Unfortunately, as seen in the image on the tissue sample, the tissue autofluorescence led to inconclusive results. The BrdU could not be deciphered to get definitive results as to the proliferation rate of cells on our scaffold. However, the presence of some BrdU fluorescence likely indicated some cell division occurring in the scaffold.

5.6 Initial Seeding Trials with Prototype

Following the scaffold verification, we wanted to test the actual capability of our device to seed cells not only on the top of the scaffold, but also within the scaffold. To do this, nine 1 cm cubes of chicken were seeded with 40k cells for both the needle device seeding method and a control submerged seeding method. Three tissue samples for each condition were examined at each time point (two days, five days, and eight days) and were sliced in half to be analyzed under the fluorescent microscope. The images in Figure 14 and Figure 15 depict these results.

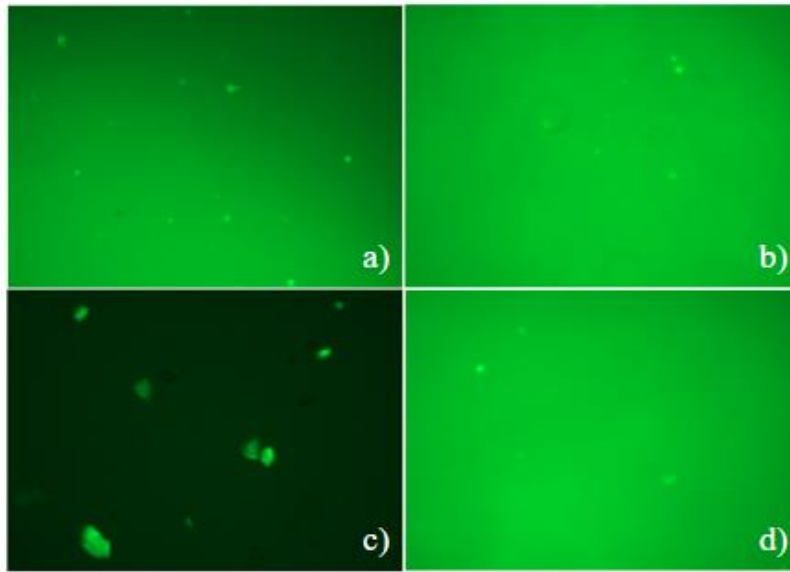


Figure 14: Day 2 images of a) submerged condition, surface of scaffold; b) submerged condition, 0.5 cm depth; c) prototype condition, surface of scaffold; d) prototype condition, 0.5 cm depth

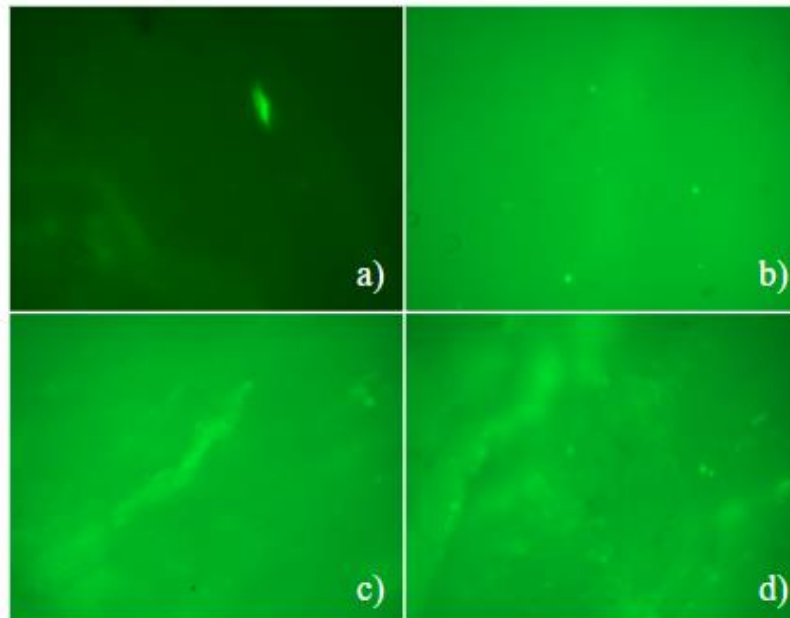


Figure 15: Day 5 images of a) submerged condition, surface of scaffold; b) submerged condition, 0.5 cm depth; c) prototype condition, surface of scaffold; d) prototype condition, 0.5 cm depth

5.7 Seeding Trial with Prototype - Higher Density

Following the initial seeding trial, it was determined that we needed to seed at a higher density in order to better observe our results. To do this, 1 cm cubes of chicken were injected with 80k cells via our device. Samples were imaged after three days using fluorescent microscopy. The following images (Figure 16) depict these results.

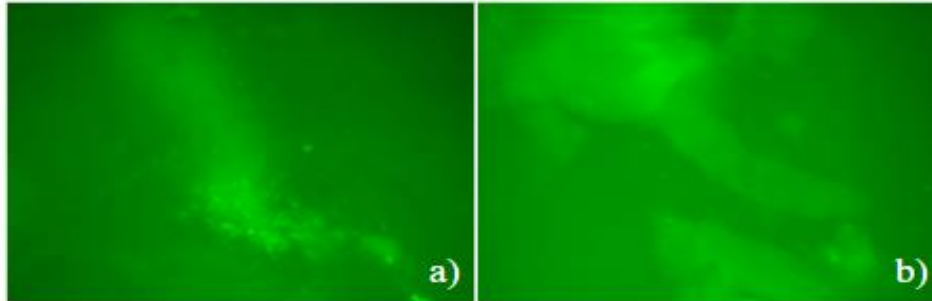


Figure 16: Higher density trial images taken on day 3 from seeding. a) surface of scaffold; b) 0.5 cm depth

5.8 Seeding Trial with Prototype - Final Trial

In our final seeding trial, three time points were tested with an even higher seeding density. Nine 1 cm cubes of chicken were injected with 1.5 million cells in 0.2 mL of complete medium via our device. Three tissue samples were examined at three time points (one day, three days, and five days) and sliced into quarters to be analyzed under the fluorescent microscope. The following images depict these results, showing cells at depths of 0, 0.25, 0.5, and 0.75 cm. This was confirmed with the green fluorescent protein expression of MDA-MB-231 cells, as well as the use of Hoechst stain to mark nuclei. The results can be seen in Figure 17 (one day), Figure 18 (three days), and Figure 19 (five days) post seeding.

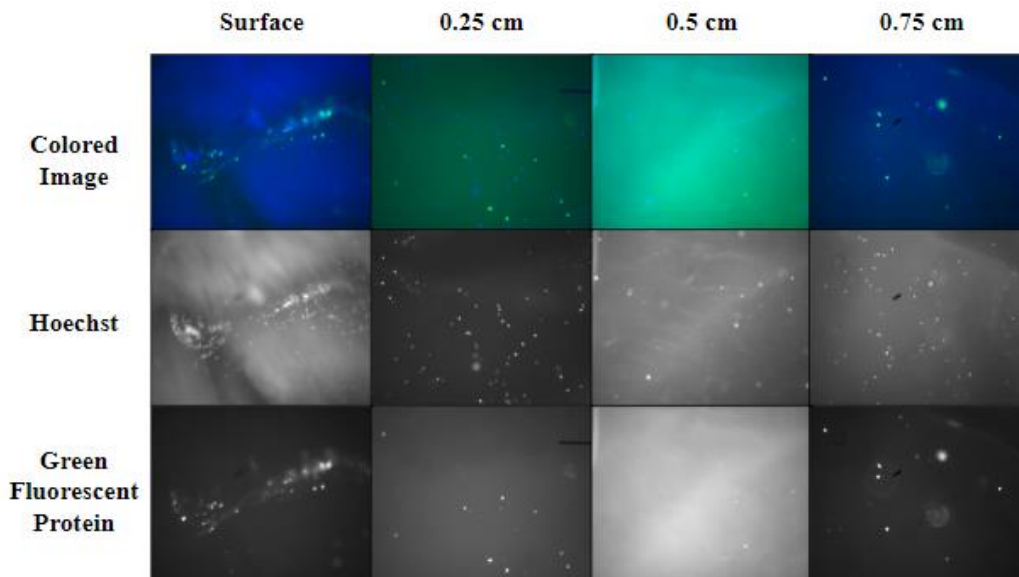


Figure 17: Final trial seeding depicting cells on scaffold one day after seeding

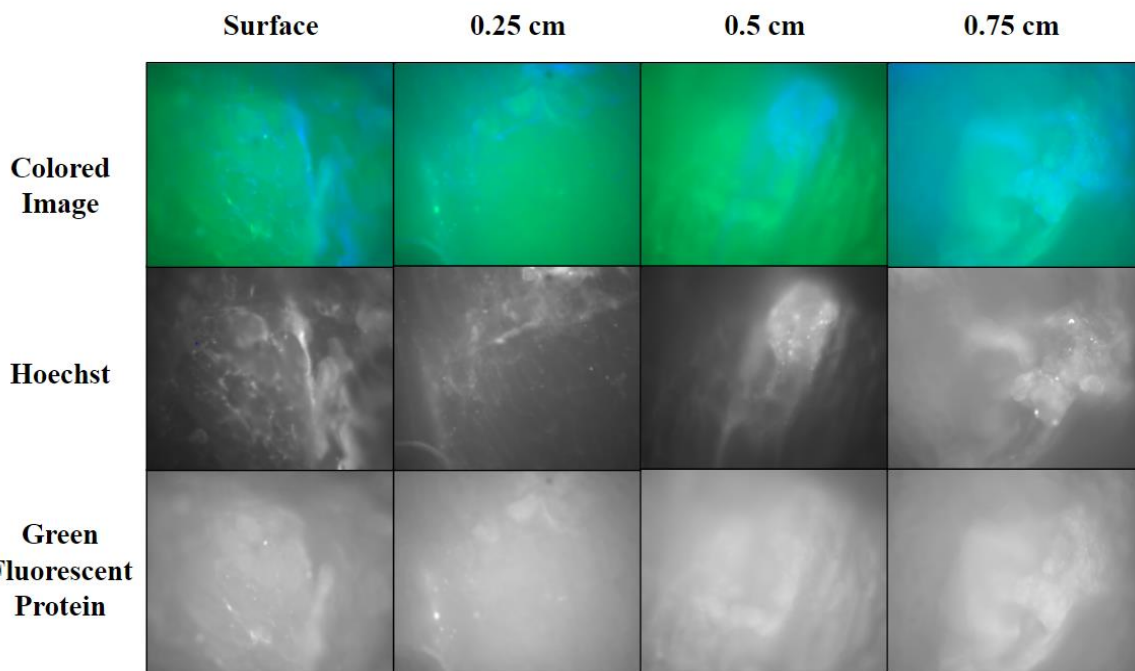


Figure 18: Final trial seeding depicting cells on scaffold three days after seeding

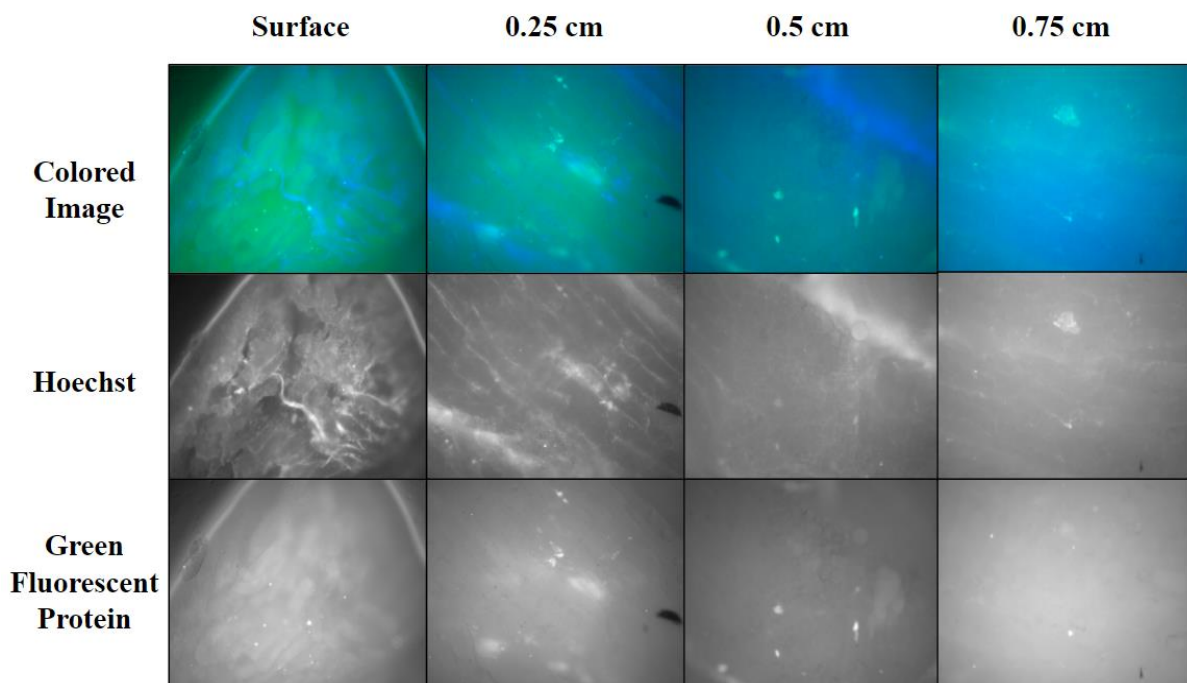


Figure 19: Final trial seeding depicting cells on scaffold five days after seeding

5.9 Final Seeding Trial - Histological Results

In the final seeding trial of the prototype. For each of the three time points (one day, three days, and five days) slices from 0.25 cm and 0.75 cm were taken from each of the tissue samples to be analyzed through histology. Figure 20 depicts the results. The purple areas in the images indicate the presence of nuclei which in turn show the presence of cells.

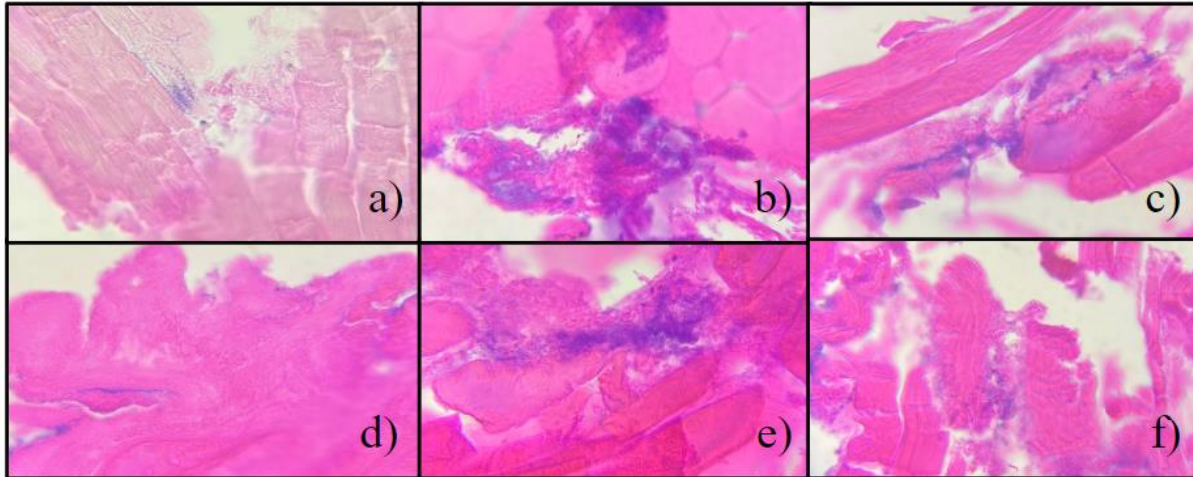


Figure 20: Final seeding histological results. a, b, and c represent 0.25 cm deep at one, three, and five days respectively from seeding. d, e, and f represent 0.75 cm deep at one, three, and five days respectively post seeding.

Chapter 6: Final Design and Validation

Decellularization

The goal for our decellularization procedure was to develop a way to fully decellularize a piece of tissue such that the structure would be maintained, biocompatible, and able to hold cells. We were able to fully decellularize our tissues as evidenced by our histological analysis which found no nuclei present on the tissues we ran through our procedure. This follows the ASTM F3354-19 Standard, as there is no nuclear material remaining under nuclear stain. Biocompatibility was also confirmed in accordance with the ISO 10993 standard for biocompatibility, as successful cell seeding means the scaffolds support cell growth. Additionally, the BrdU assay qualitatively confirmed the cells were able to survive and proliferate on decellularized scaffolds.

Cell Seeding Device

In order to achieve the 1 cm seeding depth, our final device modified and incorporated pre-manufactured stainless steel hypodermic needles. The device utilized a double platform design with springs to expose the needles at a certain length and provide a retractable mechanism. The Luer-lock mechanism was incorporated to let the device adapt to most syringes and a threaded cap was used to protect the user from exposed needles. Our prototype using 25G needles with 10 mm exposed when fully compressed was verified and validated using the dye seeding and cell seeding trials. These trials showed improved seeding with our prototype compared to static seeding, and showed cells at the surface of the scaffold, 0.25 cm, 0.5 cm, and 0.75 cm inside the scaffold. Therefore, these results can be interpreted as having successful cell seeding throughout the entirety of the scaffold.

6.1 Economics

Our decellularized scaffold has the potential to make an economic impact in that it could be purchased once and used to seed cells on multiple tissues. This would allow an off the shelf option that could detract from the cost of finding organ donors. Additionally, this device could hypothetically be used by anyone due to its cheap and simple material as opposed to other options provided by medical companies that would be overpriced for profit.

6.2 Environmental Impact

This device could be sterilized, making it usable for multiple injections. By prolonging the life of the device, it reduces the waste to the environment. Additionally, it connects to the end of any syringe, so only the needle attachment needs to be fabricated. This limits the waste caused by the manufacturing process, as well as cuts down on shipping of an additional product.

6.3 Societal Influence

The societal influence of our device comes in the form of improved quality of life for patients with myocardial infarction and potentially other conditions with large volume tissue damage. It provides a potentially more accessible approach to treating this condition. As heart disease is a leading cause of death in the US, improving patient outcomes could result in better quality of life and possibly improve life expectancy.

6.4 Political Ramifications

Our cost-effective device may enable the lobbying of medical companies and aid in providing accessible medical treatment. This may have political ramifications for for-profit medical companies.

6.5 Ethical Concerns

Ethical concerns may come into play with the cells being used with this device. Ideally this device would be used with iPSCs. However, if other types of stem cells are used that were obtained through unethical means, there may be cause for ethical concern. Additionally, a likely model for the cardiovascular system is decellularized porcine tissue. There may be people or certain cultures that would be opposed to having pig inside their bodies. On this same note, people may be opposed to having tissue originally from a different species - even if decellularized - in their bodies.

6.6 Health and Safety Issues

While our device and proposed solution may produce a tissue that allows for less of a chance of an immune rejection through the use of iPSCs, there still exists a possibility that the body will reject the foreign tissue. In regard to the device itself, it is an array of needles so there is the potential of someone accidentally injuring themselves with these needles if the device is not handled with care.

6.7 Manufacturability

The parts for the device are simple to print with the STL files and access to a moderately high resolution 3D printer. The needle assembly can be slightly difficult but could be refined such as with the use of a machine to make it easier. For mass production, the 3D printed components of the design could be molded for manufacturing and the needle components only need slight modifications on length and diameters from existing hypodermic needles manufacturing protocols. As a result, the device provides an accessible and cost-effective off the shelf option for seeding cells into tissue.

6.8 Sustainability

The device and process itself are sustainable in that it can be sterilized and used for multiple seedings. Unlike an organ transplant, which can only be used once, this device can be used multiple times to create tissues that have the potential to replace the reliance on organ donors for tissues.

Chapter 7: Discussion

7.1 Decellularization

An important component of our project was the designing of a biological scaffold onto which target cells can be seeded with our device. In order to best mimic the structure, composition, and function of native tissue, decellularization of existing tissues and organs is typically used to derive a biologic scaffold composed of ECM [4]. Through a combination of physical, chemical, and enzymatic methods, cellular material is removed from the tissues while maintaining the structural, functional, and mechanical properties of the ECM [5]. For our project, we modified a reagent-based method from an existing protocol outlined by Sesli *et al* [5].

Using the existing protocol, which calls for washes of SDS and Triton X-100, we conducted an initial trial to evaluate the effectiveness of the standard protocol against variations in reagent concentration, wash time, and conditions. For the first and second variations, the concentrations of the SDS and Triton X-100 reagents were doubled respectively. For the third variation, the amount of time the samples were placed in each reagent was doubled. And finally, for the fourth variation, a vacuum force was applied, via the vacuum chamber detailed in section 5.2, to remove air trapped in the samples and draw the reagents through the tissues. Following these treatments, the samples were analyzed using histological staining to determine which method most effectively removed the cellular material from the matrix. Upon observing the samples under a confocal microscope, we were able to determine that there were no nuclei present in any of the samples as compared with the fresh tissue control. We also observed no significant visual differences between samples, and all maintained their structure. Further analysis of the sample's mechanical properties and microstructure could be done to compare their structure preservation capabilities, however, for this initial testing, we only compared the methodologies' effectiveness in regard to the removal of cells. These results show that all variations of this methodology can provide adequate decellularization for our intended purpose, however, the adjustments made to reagent concentration, wash time, or pre-conditioning, did not significantly improve results either. Based on these findings we determined that the standard protocol would provide sufficient decellularization for our design.

The next round of scaffold experimentation was intended to standardize the decellularization protocol selected through the first round of testing. The standard protocol as outlined in the Turkish Journal of Biology did not specify the amount of reagent per sample and the rigor of rinsing between steps [5]. In order to address this ambiguity, we established a ratio of 3mL of reagent per gram of sample as the standard for reagent amount and 10 minutes as the standard for each rinse. The histological results of performing this protocol with the addition of these standards showed that while there was no evidence of nuclear material present on the exterior of the sample, there were traces of nuclear material present deeper in the tissue scaffold. No whole nuclei were observed, however, which suggests that while the cells may have been successfully broken down, the material may not have been fully washed from the tissue.

Based on the findings of our second round of testing, we assessed how increasing the number of DPBS- washes following the Triton X-100 soak affected the removal of the remaining

nuclear material. We compared the results of increasing the number of washes to three and six 10-minute washes respectively. The histological results showed that there were no cells or remaining nuclear material on the exteriors or the interiors of either sample batch. Based on these findings we determined that three 10-minute washes was sufficient to achieve the level of decellularization required for our project and finalized this method as outlined in section 5.1.

7.2 Device Design

While decellularized matrices from tissues and organs have been actively studied as a potential alternative to organ transplant for wound healing, the current recellularization techniques to deliver patient's cells into the acellular scaffold to achieve the ideal biocompatible environment are limited [21], [22]. A review by Villanoval *et al* that discusses and compares current recellularization techniques shows that despite being simple and common, static seeding has low seeding efficiency [15]. Moreover, other techniques with higher cell seeding efficiency such as rotational and centrifugal systems or magnetic and electrostatic systems may have adverse or unknown long-term effects on cell morphology and proliferation [15]. Microneedles were explored in this project as an alternative option for cell seeding based on their existing applications in drug delivery and the Clemson study's demonstration of microneedle-based recellularization protocol [10]. Despite being able to demonstrate the cell seeding capability of the microneedles prototype, the device developed in the Clemson study could not seed cells into thicker tissues [13].

The microneedle design developed in our project overcame this technical limitation, specifically the structural stability of longer needles with small diameters, by proposing a double-platform spring-loaded mechanism. While most microneedle designs available are single component, the added spring element in our design provides a retractable mechanism that stabilizes the needles as they move through the co-centric double platforms during the seeding protocol. In other words, the co-centric double platforms along with the incorporated springs help maintain the vertical movement of the needles and cells along their length while protecting the needles from any lateral movement of the tissue or human errors that may damage the thin needles. The device also includes a Luer-lock adapter to be connected with syringes loaded with cells for delivery and a threaded cap to protect the users from potential exposed needles.

Our team was able to use 25.4mm-long (1''-long) 25G hypodermic needles to produce a functional proof-of-concept prototype that exposes about 1 cm of needles when fully compressed. Originally, we intended to 3D print all components of our device, however, the resolutions on the printers available to us were not high enough to allow for this. As such, we used previously existing needles. We also considered using a vacuum chamber in conjunction with the microneedle device; however, the preliminary dye results showed that our vacuum chamber design did not have any significant seeding capacity to add to our delivery method. The India ink trial confirmed that our device could reach the desired 1 cm depth into the tissue. Its recellularization capability was confirmed with fluorescence microscopy and histology results from cell seeding trials as discussed later in the report.

Although our prototype used 25G hypodermic needles (0.51mm outer diameter and 0.26mm inner diameter) for ease of fabrication, the device is highly customizable depending on different applications. Higher gauge needles with smaller diameters could be used to minimize tissue damage. Springs could also be selected based on the spring rate desirable for the retractable mechanism. In combination, the length of the needles, the relaxed and maximum compressed length of the springs, and the length of each platform determine the exposed needle length when fully compressed, which determines the depth the device could reach, as seen in Equation 1. An additional consideration for the selection of materials seen in Equation 2 is that there should be no exposed sharp needles when the device is fully relaxed.

$$l_{\text{maximum seeding depth}} = l_{\text{needles}} - (l_{\text{bottom platform}} + l_{\text{top platform}} + l_{\text{max compressed springs}}) \quad (1)$$

$$l_{\text{relaxed spring}} + l_{\text{bottom platform}} + l_{\text{top platform}} < l_{\text{needles}} \quad (2)$$

The simple design also allows for scalability and high variability in the number and patterns of the needles and springs. As a result, future directions may include investigating the optimized needle size, number, and pattern for each tissue type. From there, additional mechanical testing could be conducted to verify that the design has appropriate mechanical properties for the specific application.

7.3 Cell Seeding

Cell seeding was essential to this project and ensured that the designed scaffold was biocompatible and that our device achieved its function. Static seeding proved that the decellularization protocol yielded biocompatible tissue, showing an abundance of cells with each injection mechanism. In Particular, Hoechst stain showed an abundance of nuclei and helped to visualize the cells without the autofluorescence of the scaffold interfering. For device validation, varying seeding densities and depths all showed cells throughout the scaffold. For the scope of this project, not all performance specifications were met quantitatively, although future works could improve seeding protocols to help aid cell adherence and increase cell density. Ideally, 90% adherence of cells to the scaffold would be achieved with maintained viability similar to that of native tissue. However, due to this being a limited proof of concept project we were unable to attempt to quantify the cell seeding results to obtain these parameters. The results we have shown indicate promise for future studies. These should include more concentration on tracking and quantifying cell adherence as well as tracking cell viability.

7.3 Study Limitations

Our study had several limitations. To begin, there were no tests to evaluate the structural integrity of the tissue following decellularization. While we confirmed the biocompatibility and ability of cells to proliferate on the scaffold, there was no testing done to see if the needles had significantly impacted the structural integrity of the existing tissue. Furthermore, the type of tissue used was limited. Chicken breast was easily accessible and cost effective, thus it was

acquired to run our studies. However, there are other kinds of tissue such as porcine cardiac tissue which may actually be more effective in our intended application in myocardial infarction as it more closely models the human heart. The cells that were used in this study were used due to their fluorescent capabilities. Ideally, however, we would use iPSCs so as to avoid an immune rejection which may or may not behave differently on our scaffold.

Regarding device design and fabrication, our project also neglected to use a vacuum chamber in conjunction with the device due to the lack of significant seeding capability of our chamber design. However, this could be a technical limitation from our vacuum chamber design and the use of other seeding techniques in conjunction with the use of our microneedle device to increase its seeding capability could be explored. As mentioned earlier, our device serves as a proof-of-concept for a spring-loaded cell delivery device and thus, optimization and mechanical testing may be needed to adapt the design to specific applications. Lastly, our study was limited by the 3D printers and fabrication techniques available to us. Due to the fact that the resolution was not high enough, we were unable to print needles small enough to fit our specifications. As such, we had to devise a device using preexisting needles as opposed to creating our own.

Chapter 8: Conclusions and Recommendations

This project demonstrates proof of concept for a viable, off-the-shelf tissue scaffold for large volume tissue injuries. The development of a decellularization protocol led to successful verification of decellularization through histology. The scaffold was confirmed to be biocompatible through static cell seeding. A microneedle device was then designed to successfully inject cells into tissue of 1 cm thickness, with controlled dispersion of cells. This depth was verified using a fluorescent microscope. In summary, this shows that a device of spring-loaded needles can be used to seed cells into deeper tissue, such as cardiac tissue.

This decellularization, reseeding process and device could be implemented to make grafts and treatments for diseases such as myocardial infarction. By replacing damaged tissue, patient outlook and life expectancy could increase. Currently, treatment options for myocardial infarction are limited by the number of organ donors, and other treatments result in loss of mobility or function in other areas of the body. Scalability of this design and process could improve treatment and replace the need for organ donations or cardiac bypass surgery. Additionally, the ability to use autologous cells would limit the chance for immune rejection with a graft or transplant, reducing the risks associated with treatment.

This project was limited specifically to chicken breast in the decellularization and reseeding process, primarily due to cost and obtainability. Prior to treatments, these protocols should be tested in other models. Ideally, porcine cardiac tissue could be used, due to the similarity between the pig and human cardiovascular systems. It is also recommended to test the seeding efficiency of additional cell types. Specifically, iPSCs could be used for treatment options, which would reduce the risk of immune rejection in patients. Additionally, device design could improve in order to facilitate device production. While this project was limited to the printing resolution of a Form2 printer, a printer with better resolution could make a more precise device. Additionally, improving the process of adding the needles to the device should be done. This is recommended to be done automatically, as the needles pose safety hazards for workers. Finally, this device could be modified to penetrate even deeper tissue by simply changing the needle length and resistance to the springs, expanding the possible applications of the device.

In conclusion, this report serves to show proof of concept that an off-the-shelf decellularized scaffold can be seeded with cells through the use of a spring-loaded needle array. By seeding patient-specific cells onto the scaffold, it reduces the risk of immune rejection. This process and device function to create a viable treatment for large volume tissue injuries. The wound healing implications have the potential to improve treatment options for patients, thus improving patient outcomes, quality of life, and possibly life expectancy.

References

- [1] “Tissue Engineering and Regenerative Medicine,” *National Institute of Biomedical Imaging and Bioengineering*. <https://www.nibib.nih.gov/science-education/science-topics/tissue-engineering-and-regenerative-medicine> (accessed Nov. 10, 2021).
- [2] H. Kaul and Y. Ventikos, “On the Genealogy of Tissue Engineering and Regenerative Medicine,” *Tissue Eng. Part B Rev.*, vol. 21, no. 2, pp. 203–217, Apr. 2015, doi: 10.1089/ten.teb.2014.0285.
- [3] M. J. Buckenmeyer, T. J. Meder, T. A. Prest, and B. N. Brown, “Decellularization techniques and their applications for the repair and regeneration of the nervous system,” *Methods*, vol. 171, pp. 41–61, Jan. 2020, doi: 10.1016/j.ymeth.2019.07.023.
- [4] P. M. Crapo, T. W. Gilbert, and S. F. Badylak, “An overview of tissue and whole organ decellularization processes,” *Biomaterials*, vol. 32, no. 12, Art. no. 12, Apr. 2011, doi: 10.1016/j.biomaterials.2011.01.057.
- [5] M. SESLİ, E. AKBAY, and M. A. ONUR, “Decellularization of rat adipose tissue, diaphragm, and heart: a comparison of two decellularization methods,” *Turk. J. Biol.*, vol. 42, no. 6, Art. no. 6, Dec. 2018, doi: 10.3906/biy-1807-109.
- [6] “American Heart Association | To be a relentless force for a world of longer, healthier lives.” <https://www.heart.org/> (accessed Oct. 04, 2021).
- [7] “Coronary Artery Bypass Graft Surgery,” Oct. 04, 2021. <https://www.hopkinsmedicine.org/health/treatment-tests-and-therapies/coronary-artery-bypass-graft-surgery> (accessed Oct. 04, 2021).
- [8] A. Futakuchi-Tsuchida and C. E. Murry, “Human myocardial grafts: do they meet all the criteria for true heart regeneration?,” *Future Cardiol.*, vol. 9, no. 2, Art. no. 2, Mar. 2013, doi: 10.2217/fca.13.8.
- [9] P. KC, Y. Hong, and G. Zhang, “Cardiac tissue-derived extracellular matrix scaffolds for myocardial repair: advantages and challenges,” *Regen. Biomater.*, vol. 6, no. 4, pp. 185–199, Aug. 2019, doi: 10.1093/rb/rbz017.
- [10] J. Yang, X. Liu, Y. Fu, and Y. Song, “Recent advances of microneedles for biomedical applications: drug delivery and beyond,” *Acta Pharm. Sin. B*, vol. 9, no. 3, Art. no. 3, May 2019, doi: 10.1016/j.apsb.2019.03.007.
- [11] H. Rezaei Nejar, A. Sadeqi, G. Kaiee, and S. Sonkusale, “Low-cost and cleanroom-free fabrication of microneedles,” *Mycrosystems Nanoeng.*, vol. 4, p. 17073, 2018.
- [12] Sajjad Rahmani Dabbagh, Misagh Rezapour Sarabi, Reza Rahbarghazi, Emel Sokullu, Ali K. Yetisen, and Savas Tasoglu, “3D-printed microneedles in biomedical applications,” *IScience Cell Press*, vol. 24, p. 102012, 2021.
- [13] M. Rye, “Microneedle Arrays for Injection Seeding of Tissue Engineered Scaffolds,” *TigerPrints*, vol. AllTheses, 2014, [Online]. Available: https://tigerprints.clemson.edu/cgi/viewcontent.cgi?article=3508&context=all_theses
- [14] Y. Guo *et al.*, “Culturing of ventricle cells at high density and construction of engineered cardiac cell sheets without scaffold,” *Int. Heart. J.*, vol. 50, no. 5, Art. no. 5, Sep. 2009, doi: 10.1536/ihj.50.653.
- [15] G. A. Villalona *et al.*, “Cell-seeding techniques in vascular tissue engineering,” *Tissue Eng. Part B Rev.*, vol. 16, no. 3, pp. 341–350, Jun. 2010, doi: 10.1089/ten.TEB.2009.0527.

- [16] S. F. Badylak, D. Taylor, and K. Uygun, “Whole-Organ Tissue Engineering: Decellularization and Recellularization of Three-Dimensional Matrix Scaffolds,” *Annu. Rev. Biomed. Eng.*, vol. 13, no. 1, Art. no. 1, Aug. 2011, doi: 10.1146/annurev-bioeng-071910-124743.
- [17] S. Economidou, C. P. Pissinato Pere, M. Okereke, and D. Douromis, “Optimisation of Design and Manufacturing Parameters of 3D Printed Solid Microneedles for Improved Strength, Sharpness, and Drug Delivery,” *Micromechanics*, vol. 12, no. 2, p. 117, 2021.
- [18] Subcommittee F04.44, “ASTM F3368-49, Standard Guide for Cell Potency Assays for Cell Therapy and Tissue Engineered Products,” *ASTM International*, 2019. <https://www.astm.org/Standards/F3368.htm> (accessed Nov. 10, 2021).
- [19] N. N. Ahmad, N. N. N. Ghazali, and Y. H. Wong, “Concept Design of Transdermal Microneedles for Diagnosis and Drug Delivery: A Review,” *Adv. Eng. Mater.*, Jun. 2021, Accessed: Nov. 10, 2021. [Online]. Available: <https://onlinelibrary.wiley.com/doi/full/10.1002/adem.202100503>
- [20] “ASTM F3354-19, Standard Guide for Evaluating Extracellular Matrix Decellularization Processes,” *ASTM International*, 2019. <https://www.astm.org/Standards/F3354.htm> (accessed Nov. 10, 2021).
- [21] Doris A. Taylor, Luiz C. Sampaio, Zannatul Ferdous, Andrea S. Gobin, and Lakeshia J. Taite, “Decellularized matrices in regenerative medicine,” *Acta Biomater.*, vol. 74, pp. 74–89, Jul. 2018, doi: 10.1016/j.actbio.2018.04.044.
- [22] Xuewei Zhang, Xi Chen, Hua Hong, Rubei Hu, Jiashang Liu, and Changsheng Liu, “Decellularized extracellular matrix scaffolds: Recent trends and emerging strategies in tissue engineering,” *Bioact. Mater.*, vol. 10, pp. 15–31, doi: 10.1016/j.bioactmat.2021.09.014.

Appendix A

Histology Procedure:

1. Samples were sectioned into 0.25 cm slices and placed in cassettes.
2. Cassettes were placed in a 4% formalin solution and left overnight.
3. Samples were processed in a tissue processor.
4. Following processing, samples were embedded in paraffin wax and left to cool.
5. Embedded samples were then sectioned with a microtome in 10 micron slices.
6. Sections were carefully placed in a water bath of 40 degrees C before being scooped up onto a slide.
7. Slides were left to dry in the slide warmer overnight.
8. The slides were stained with hematoxylin and eosin in the following procedure:
 - a. Xylene - 3 mins
 - b. Xylene - 3 mins
 - c. Xylene - 3 mins
 - d. 100% ETOH - 3 mins
 - e. 100% ETOH - 3 mins
 - f. 95% ETOH - 1 min
 - g. 70% ETOH - 1 min
 - h. Rinse in H₂O - ~5 mins
 - i. Harris Hematoxylin (filter before and after use) - 5 mins
 - j. Rinse in H₂O - ~5mins
 - k. Differentiate in acid alcohol - 2-3 quick dips
 - l. Rinse in H₂O - 30 secs
 - m. Blue sections in ammonia water - 1 min
 - n. Rinse in H₂O - 5 mins
 - o. 95% ETOH - 1 min
 - p. Counterstain in Eosin Y - 1 min
 - q. 95% ETOH - 30 secs
 - r. 95% ETOH - 30 secs
 - s. 100% ETOH - 1 min
 - t. 100% ETOH - 1 min
 - u. 100% ETOH - 1 min
 - v. Xylene - 1 min
 - w. Xylene - 1 min
 - x. Xylene - 1 min
9. Coverslip the stained slides and analyze.

Appendix B

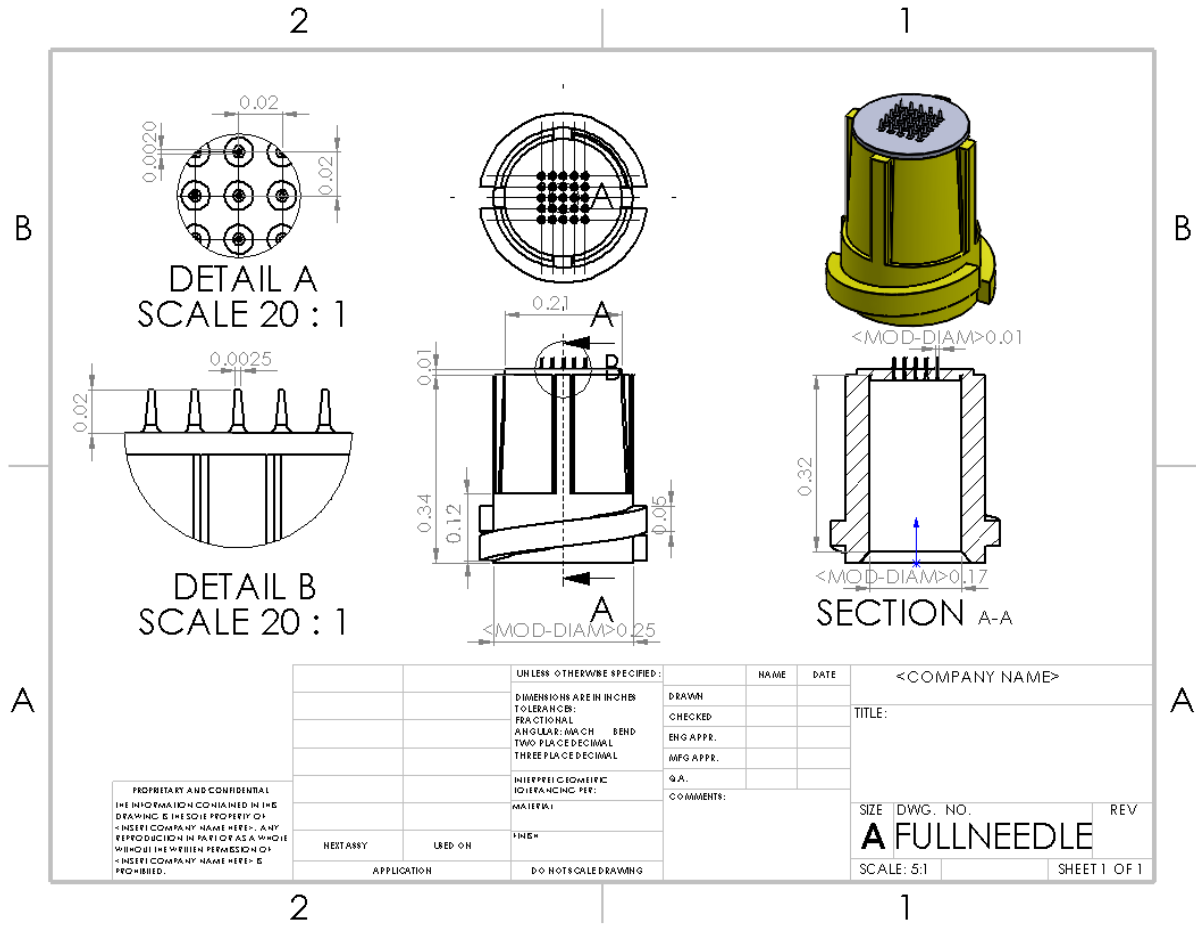


Figure 21: Detailed CAD drawing of the first needle design.

Appendix C

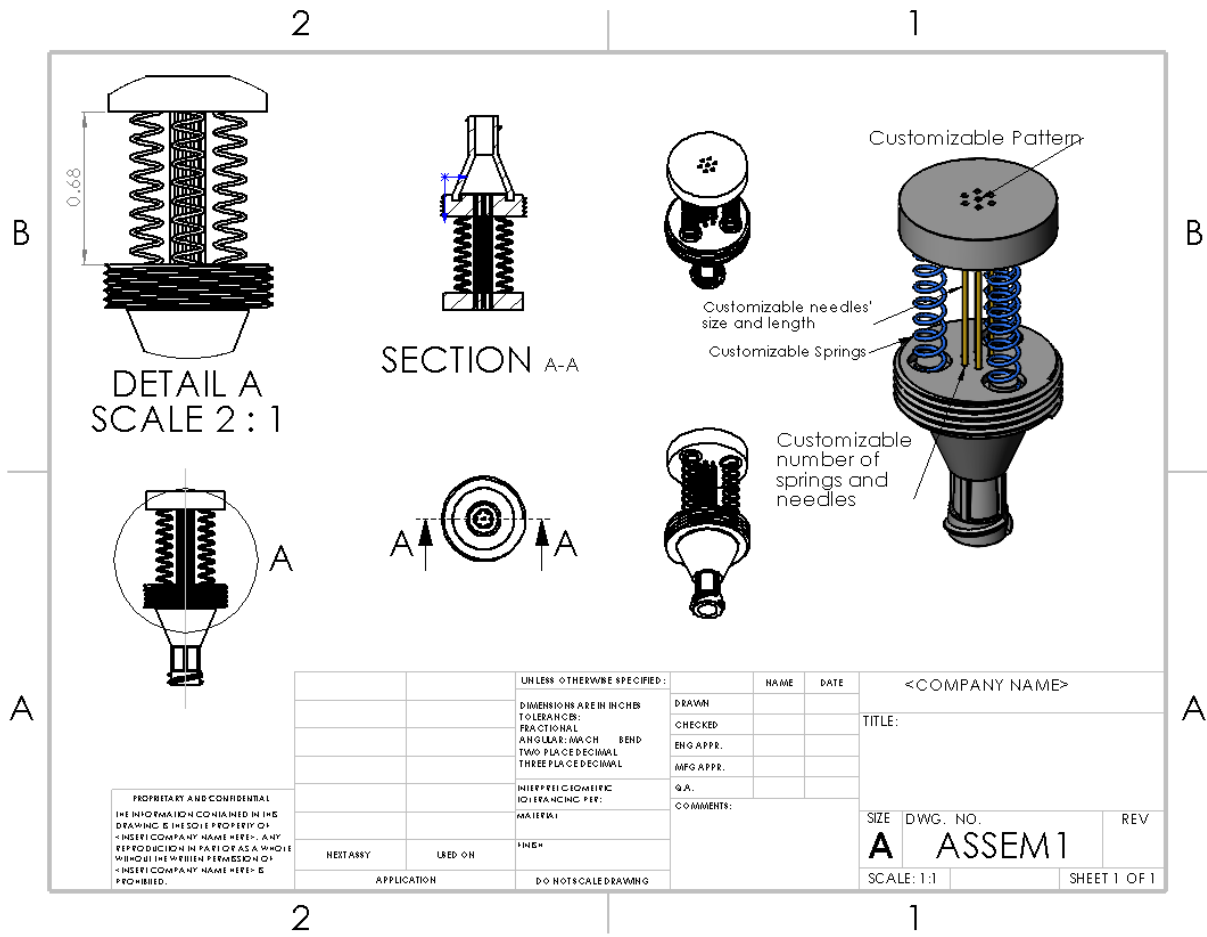


Figure 22: Detailed CAD drawing of the final microneedle design device assembly.

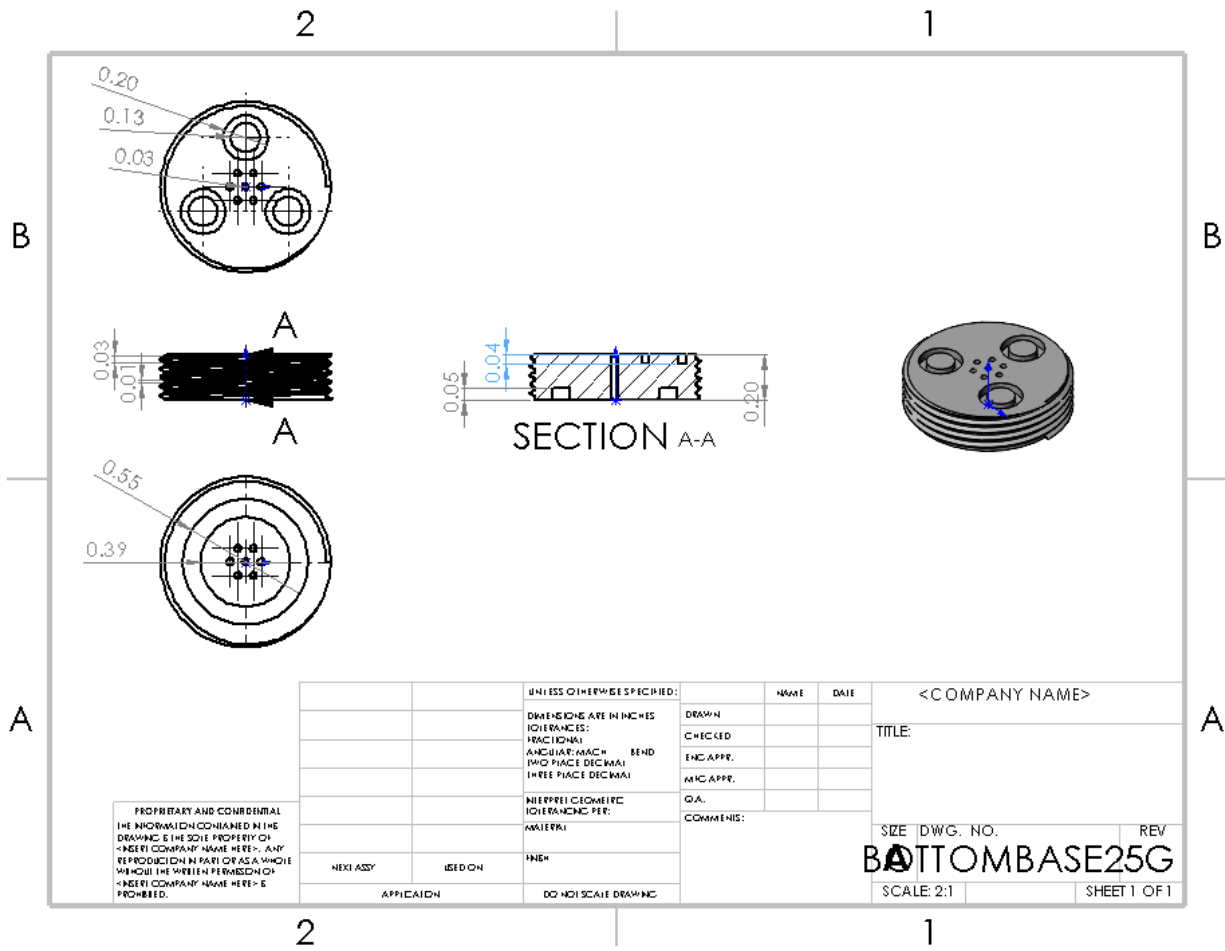


Figure 23: Detailed CAD drawing of the bottom base component of the final microneedle design device assembly.

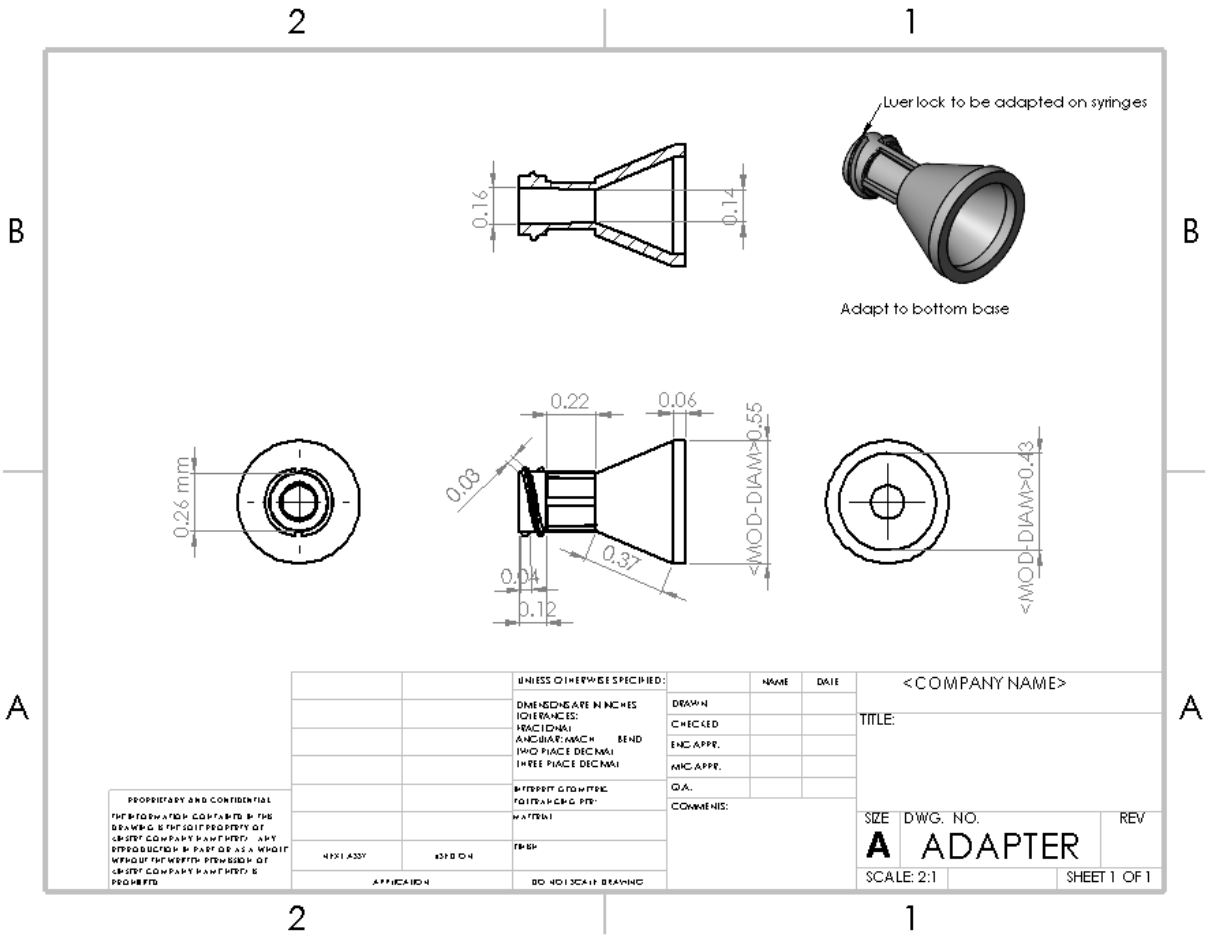


Figure 24: Detailed CAD drawing of the adapter component of the final microneedle design device assembly.

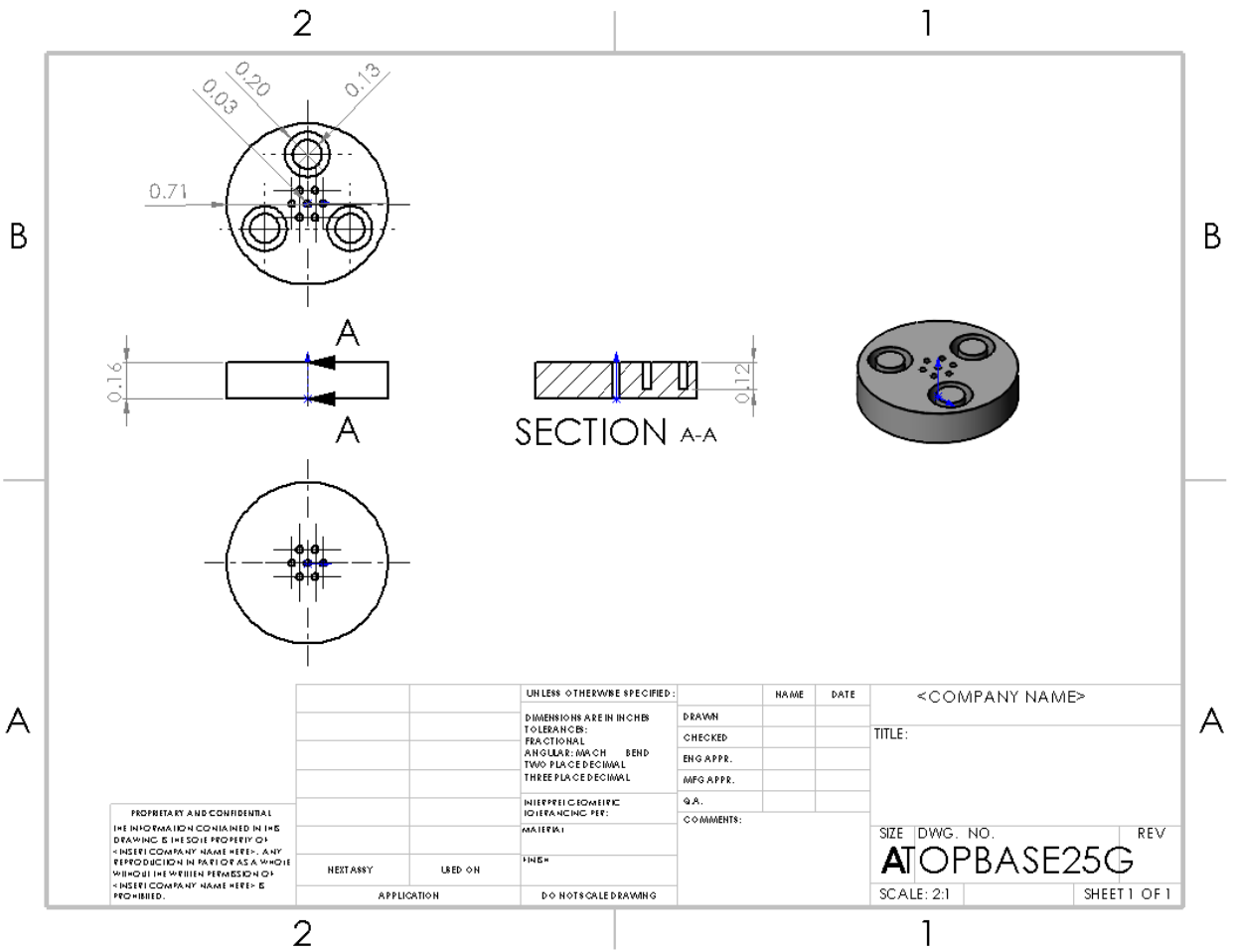


Figure 26: Detailed CAD drawing of the top base component of the final microneedle design device assembly.